Exhaust gas recirculation on twin shaft gas turbines

A study to improve part load performance

Benjamin Mattsson

LUND
UNIVERSITY

April 2015
Thesis for the degree of Master of Science
Division of Thermal Power Engineering
Department of Energy Sciences
Lund University, Sweden

Division of Thermal Power Engineering
Department of Energy Sciences
Lund University
P.O. Box 118
SE-221 00 Lund
Sweden

ISRN LUTMDN/TMHP-15/5330-SE
ISSN 0282-1990

Printed in Sweden by E-huset Tryckeri
Lund 2015

to Tuva

Abstract

By recirculating exhaust gases to the gas turbine inlet a temperature rise and hence, a density reduction, is achieved at the compressor inlet. For a constant volume flow this results in a reduced mass flow, ultimately affecting the temperature of the flame, and the emissions, at part load. This study is conducted by creating a model of the Siemens twin shaft gas turbine SGT-750 in the software IPSEpro. The model is based on characteristics which are read from a text file. With the model, different cases of exhaust gas recirculation, EGR, are examined and the calculations are carried out for a simple as well as a combined cycle. Both cycles are examined with standard and tropical ambient conditions and matching.

Depending on the case studied the results yield a $3-5$ percentage point increase in total cycle efficiency at $50\,\%$ load compared to the method of bleed used today. Furthermore, the gas turbine performance is better at normal conditions comparatively and the limitations of temperature and rotational speed is reached at higher loads for the tropical match. Although negative effects such as influence on lifing and practical issues of implementation are present, EGR is recommended based on the positive results and the general improvement of the gas turbine performance with the method.

Key words: Exhaust gas recirculation, EGR, FGR, Twin shaft gas turbine, Part load, Emissions, SGT-750, IPSEpro, SimTech.

Preface

This thesis for the degree of Master of Science in Mechanical Engineering marks the end of my five year education at the Faculty of Engineering, Lund University. The work has been conducted from late November 2014 to April 2015 at Siemens Industrial Turbomachinery AB in Finspång, Sweden.

First and foremost I would like to thank Klas Jonshagen, my supervisor at Siemens. Over the nearly five months of time we have been working together you have not once been unable to help or guide me through the process. We have formed a great team solving our shared challenges and my contribution has felt meaningful.

I would also like to thank everyone in the RGP department for making me feel welcome and special thanks to Kerstin Tageman for enduring all my questions and issues regarding the SGT-750.

Thanks also to my supervisor Magnus Genrup and examiner Marcus Thern at the department of Energy Sciences, Lund University, for supporting me throughout this project as well as through my whole specialization.

Finally I would like to thank my family and loved ones for all support.

Benjamin Mattsson
Finspång, 2015-04-07

Nomenclature

Arabic symbols	Description	Unit
A	Area	m^2
AS	Aero speed	–*
c	Absolute velocity	m/s
CT	Flow capacity	–*
D	Diameter	m
f	Friction factor	–
h	Enthalpy	kJ/kg
K_L	Loss coefficient	–
l	Length	m
$\dot{m}$	Mass flow	kg/s
Ma	Mach number	–
N	Rotational speed	rpm
p	Pressure	bar
P	Power	MW
$\dot{Q}$	Heat flux	kW
R	Gas constant	kJ/(kg K)
Re	Reynolds number	–
s	Entropy	kJ/(kg K)
T	Temperature	°C / K
u	Blade velocity	m/s
v	Velocity	m/s
w	Relative velocity	m/s
$\dot{W}$	Power	kW
X/x	Arbitrary variable	–

*Unit irrelevant, not dimensionless.

Greek symbols	Description	Unit
γ	Isentropic exponent	–
Δ	Finite difference	–
ε	Equivalent roughness	m
η	Efficiency	–
θ	Tangential value	–
μ	Dynamic viscosity	Pa s
π	Pressure ratio	–
ρ	Density	kg/m^3
σ	Stress	N/m^2

Subscripts	Description
0	Total value
amb	Ambient
corr	Corrected
EGR	Exhaust gas recirculation
exh	Exhaust
fric	Friction
gen	Generator
in	Input
lam	Laminar
loss	Power loss
out	Output
n	Arbitrary state
net	Net value
ref	Reference
rel	Relative
s	Isentropic
turb	Turbulent
x	Axial

SIT specific subscripts	Description
0100	Gas turbine inlet
0500	Power turbine inlet
0850	Gas turbine exhaust before pressure drop
0950	Gas turbine exhaust after pressure drop
1200	Compressor inlet
1300	Compressor outlet
1500	Compressor turbine inlet
1520	Fictitious compressor turbine inlet after mixed with cooling air
3450	Flame

Abbrevations	Description
CCS	Carbon capture and storage
DLE	Dry low emissions
DLL	Dynamic link library
DN	Nominal diameter
EGR	Exhaust gas recirculation
FAR	Fuel to air ratio
FGR	Flue gas recirculation
GG	Gas generator
GTP	GTPerform
HRSG	Heat recovery steam generator
IEEE	Institute of Electrical and Electronics Engineers
IGV	Inlet guide vane
ISO	International Organization for Standardization
MDK	Model development kit
SAS	Secondary air system
SGT	Siemens gas turbine
SIT	Siemens Industrial Turbomachinery AB
STAL	Svenska Turbinfabriks Aktiebolaget Ljungström
TIT	Turbine inlet temperature
VGV	Variable guide vane

Contents

List of Figures

List of Tables

1

Introduction

Finspång has played an important role in the industrial heritage of Sweden ever since Louis De Geer started the production of cannons in the town in 1631 [1]. Since the steam turbine production was initiated in 1913, under the name of STAL, the site has been a center of turbine development leading to the company of today, Siemens Industrial Turbomachinery AB, being at the cutting edge of gas turbine technology. The gas turbines manufactured at SIT are under constant development and at the site the entire chain of production is present, from research, development and project planning to manufacturing, delivery and maintenance services.

1.1 Background

Earth's climate change is one of the greatest challenges of our time. A challenge that has made the development of renewable energy sources, as for example solar and wind power, increase rapidly. With expanding intermittent energy sources, as those mentioned, in the power grid the need for fast regulated balance power increases. Since gas turbines are relatively fast regulated and also most often installed in smaller power plants they are an attractive form of balancing power. Furthermore, twin shaft gas turbines are widely used for mechanical drive, a case that puts high demands on an efficient process at part load. Conclusively, gas turbine manufacturers are facing a future were performance at part load is of increasing importance and needs to improve to meet the requests and demands of the market.

1.2 Objectives

This work is expected to sort out the possibilities of reducing the load and increase the efficiency and overall performance without adversely affect the emissions on twin shaft gas turbines. This is to be made with exhaust gas recirculation, henceforth abbreviated EGR. The study will be conducted with the Siemens twin shaft gas turbine SGT-750 as an example. The model constructed during the process will also serve as the company's standard model in the software IPSEpro for SGT-750. In summary the work process will mainly revolve around the following points.

- Construction of a model of the SGT-750 in IPSEpro.
- Development of DLL file for IPSEpro to read Siemens component characteristics from text files.
- Validation of the model's calculations against Siemens performance programs to ensure its accuracy.
- Using the model to investigate and analyze the impact and potential of EGR under the following circumstances.
  1. Simple cycle
     (a) At ISO conditions with normal match.
     (b) At tropical conditions with tropical match.
  2. Combined cycle
     (a) At ISO conditions with normal match.
     (b) At tropical conditions with tropical match.

1.3 Limitations

There are a lot of aspects to consider when implementing EGR in a gas turbine cycle. This thesis will primarily focus on the thermodynamic ones. While other aspects are present, the following will not be considered in the work.

- The analysis will regard steady state calculations and hence, no transient analysis will be performed.
- Solid mechanics will not be examined and hence, no extensive lifing analysis will be conducted. Only specific physical limits will be considered.
- While some practical issues with EGR will be discussed, this is to be considered a preliminary study and no in depth analysis of the practicalities will be performed.
- No particular economic aspects will be taken into account although the gas turbine's efficiency will be studied and evaluated, a factor that can be directly linked to financial aspects.

1.4 Outline

Chapter 1
Chapter 1 contains a general introduction. The thesis is introduced with a background to the problem and its objectives are clearly specified. Furthermore, the general limitations of the thesis are presented.

Chapter 2
In Chapter 2 the theory needed to fulfill the thesis' purpose is presented. Note that a basic level of knowledge within the field of thermodynamics and turbomachinery is expected from the reader since only the specific theory required for the thesis is presented. For a more general theory the cited references are recommended.

Chapter 3
Chapter 3 covers the methodology of the thesis in detail. All the steps in the process of developing the model are presented, as well as how the analysis was performed.

Chapter 4
The results of the analysis are presented and commented in Chapter 4. The analyzed cases are compared mainly by examining key parameters with varied load.

Chapter 5
In Chapter 5 the discussion is covered where the results are analyzed from a more general point of view. Also, a conclusion is determined and presented together with a review of the occurring sources of error, as well as the further work within the subject.

References
The chapter References contains a list of all cited works in a slightly modified version of the IEEE citation style. The references are general throughout the thesis with the exception of pure definitions that are cited with page numbers.

Appendices
The thesis contains two appendices. In Appendix A an extract of the DLL code written is presented while Appendix B contains complementary results of the model validation.

2

Theory

A gas turbine's working principle is that a compressor compresses air after which fuel is injected and burned. The pressurized combustion air, now of high temperature and enthalpy, is expanded through a turbine which transforms the energy into mechanical work. The turbine's mechanical work, excluding losses, drives the compressor and the excess energy is used to drive a load. In electric generation as focused on in this thesis, the load consists of a generator. A schematic illustration of a single shaft gas turbine is presented in Figure 2.1.

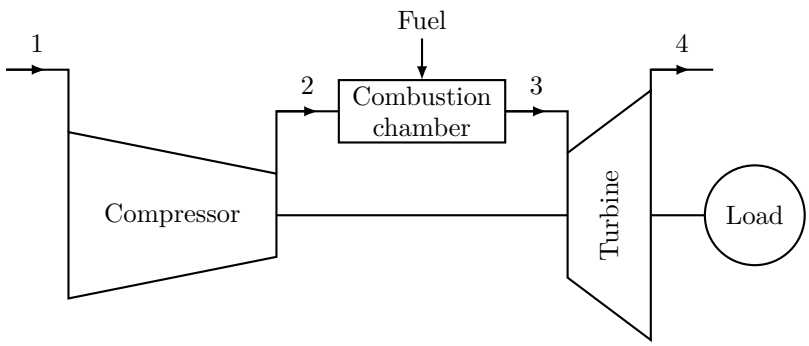

Figure 2.1. Schematic illustration of a single shaft gas turbine.

2.1 Twin shaft gas turbines

Twin shaft gas turbines are different, from single shaft machines, in the fact that they are running two turbines with mechanically separated shafts. The first one, the compressor turbine, is as with single shaft gas turbines connected to the compressor. This turbine produces the exact amount of energy the compressor requires, with losses taken into account. This first part of the twin shaft gas turbine is often referred to as the gas generator. After the gas generator the combustion air is led to a second turbine, the free power turbine. Here the excess energy is transformed into mechanical work and used to drive the load through a separate second shaft and possibly a gear box. With no mechanical connection to the compressor, the free power turbine is independent and is for example able to run at a shaft speed unrelated to other parts of the engine. Due to this the machine type is useful to drive a varied load, the twin shaft gas turbine's main advantage. Another benefit from using separated shafts is, as Cohen *et al.* [2] describes, that the torque is high at low shaft speeds, a useful property when using a gas turbine for vehicle operation. A schematic illustration of a twin shaft gas turbine is presented in Figure 2.2.

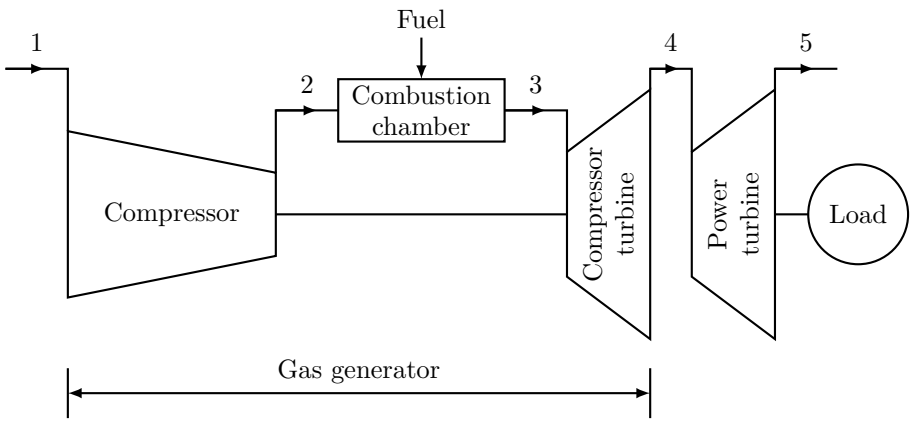

Figure 2.2. Schematic illustration of a twin shaft gas turbine.

Despite the lack of mechanical coupling between the compressor and power turbine, there is an existing coupling called aerothermal (aero- and thermodynamic) between the two. This means the components are not as independent as can be adopted at first glance. The phenomenon affects the matching and interaction between components and has to be considered in the process of calculating a twin shaft gas turbine.

On multiple shaft gas turbines the power turbine can be differently matched. With a VGV, the power turbine is optimized depending on the prevailing ambient conditions. The SGT-750 can be matched for normal and tropical conditions.

2.1.1 SGT-750

The SGT-750, Figure 2.3, is the company's latest addition to the product portfolio. Due to its twin shaft configuration and power output of approximately 38 MW it is a versatile gas turbine, suitable for numerous applications such as simple cycle, combined cycle and mechanical drive. With DLE technology, NO_x emissions are kept below 15 ppm_v, Siemens AG [3], although emissions remain an issue at part load.

Today emissions at part load are controlled by bleeding pressurized air from after the compressor to the gas turbine exhaust. Seen from a performance point of view this is the worst possible approach although not to belittle, the easiest and cheapest one. Tageman [4] describes the alternatives and why this inefficient method was chosen in the development process. The bleed method could be made with bleed to the compressor inlet but problems occurred with mixing the high pressure air with the ambient. Bypassing air over the burners is a possible solution but was rejected due to the can burner setup. Ultimately bleed to the exhaust was chosen due to its simplicity, robustness and low cost.

Further Tageman [4] describes the way the amount of bleed air is controlled. It is done by aiming for a target value of T_{1520} with the load lowered until this target value is reached. At further lowered load, T_{1520} is kept constant as a result of gradually opening the bleed valve allowing pressurized air to be dumped and thus, reducing the burner mass flow. At a bleed mass fraction exceeding a limit, T_{1520} is lowered further until the lower bound of the temperature, due to emission requirements, is reached.

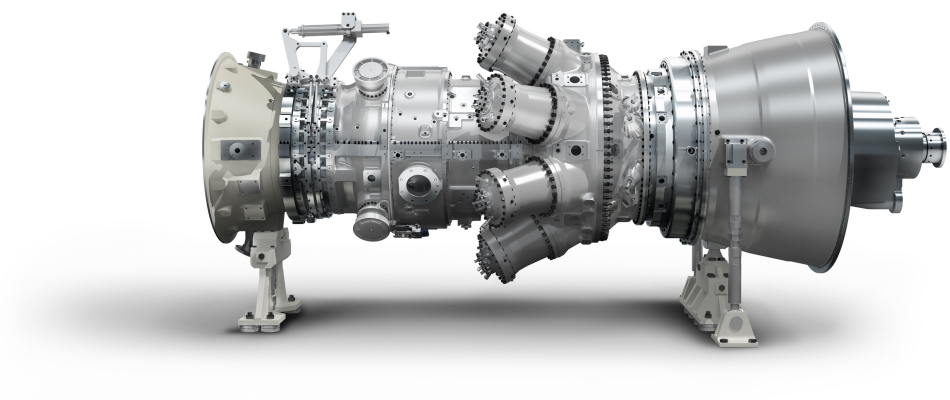

Figure 2.3. Computer rendered illustration of the SGT-750, Siemens Industrial Turbomachinery AB [5].

2.2 General thermodynamics

Some general thermodynamic relations and theory needed to proceed with the theory of this thesis is presented below.

2.2.1 Cycle efficiency and the ideal Brayton cycle

The ideal cycle for gas turbine engines was invented by George Brayton, hence it is called the ideal Brayton cycle. The thermal efficiency of an ideal Brayton cycle may be defined in accordance to Çengel and Boles [6, p.471], with notations stated in Table 2.1 and Figure 2.1.

$$\eta = \frac{\dot{W}_{net,out}}{\dot{Q}_{in}} = \frac{(h_3 - h_4) - (h_2 - h_1)}{(h_3 - h_2)} \tag{2.1}$$

Table 2.1. Notations for the ideal Brayton cycle.

1. Before compression
2. After compression
3. Before expansion
4. After expansion

Assuming constant specific heat capacity the expression is rewritten.

$$\eta = \frac{(T_3 - T_4) - (T_2 - T_1)}{(T_3 - T_2)} = 1 - \frac{(T_4 - T_1)}{(T_3 - T_2)} = 1 - \frac{T_1\,(\frac{T_4}{T_1} - 1)}{T_2\,(\frac{T_3}{T_2} - 1)} \tag{2.2}$$

The thermal efficiency is rewritten as a function of pressure ratio and isentropic exponent using isentropic relations. This is made assuming both the compression and expansion process to be isentropic and no pressure loss to occur in between, that is $p_1 = p_4$ and $p_2 = p_3$.

$$\frac{T_2}{T_1} = \left(\frac{p_2}{p_1}\right)^{\frac{\gamma-1}{\gamma}} = \pi^{\frac{\gamma-1}{\gamma}} = \left(\frac{p_3}{p_4}\right)^{\frac{\gamma-1}{\gamma}} = \frac{T_3}{T_4} \tag{2.3}$$

$$\eta = 1 - \frac{1}{\pi^{\frac{\gamma-1}{\gamma}}} = f(\pi, \gamma) \tag{2.4}$$

2.2.2 Isentropic versus polytropic efficiency

Consider a compression process from p_a to p_c, according to Figure 2.4. The isentropic efficiency handles the compression as a linear process while in reality, a more accurate way to describe it is with the polytropic efficiency as a non-linear polynomial. Calculating a part process, in example a compression from p_a to p_b, using the polytropic effiency will result in the more accurate result of b'' instead of b'.

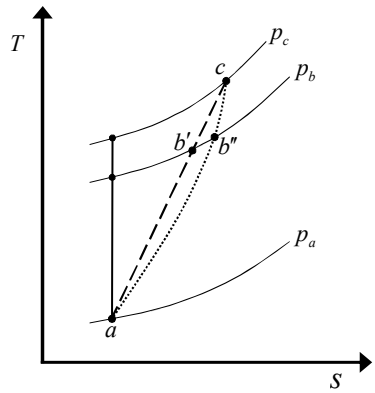

Figure 2.4. Comparision of isentropic and polytropic efficiency.

2.2.3 Pipe pressure loss

Pressure losses due to friction in pipes and ducts are called major losses while the minor losses consists of losses due to specific components, such as valves and bends. The total pressure loss, including both major and minor losses, is defined by the Darcy–Weisbach equation according to Young *et al.* [7].

$$\Delta p_{fric} = \left(\frac{f\,l}{D} + \sum K_L \right) \frac{\rho\, v^2}{2} \tag{2.5}$$

The friction loss factor for laminar flows is described by Young *et al.* [7]. For turbulent flows a dependence of relative roughness, ε/D, is present and the friction loss factor can be approximated with the Haaland equation according to Haaland [8].

$$f_{lam} = \frac{64}{Re} \tag{2.6a}$$

$$\frac{1}{\sqrt{f_{turb}}} = -1.8 \cdot \log_{10} \left[\left(\frac{\varepsilon/D}{3.7} \right)^{1.11} + \frac{6.9}{Re} \right] \tag{2.6b}$$

Young *et al.* [7] describes a flow to be laminar if the Reynolds number is below approximately 2100 and turbulent if above 4000. Reynolds number is defined as follows were the velocity is calculated with the mass flow rate in Equation 2.9.

$$Re = \frac{\rho\, v\, D}{\mu} \tag{2.7}$$

2.3 Performance prediction

A gas turbine's performance at all operating conditions depends on numerous describing parameters, as for example ambient temperature and pressure, rotational speed, IGV angle, gas constant etcetera. The large number of parameters can make the performance difficult to interpret. A way to reduce the number of parameters is to create parameter groups to make the information more perspicuous and also facilitate further calculations. In an example Walsh and Fletcher [9] describes a reduction from eight parameters to three parameter groups. These parameter groups can be derived using either dimensional analysis, as for example the Buckingham pi theorem, or by creating velocity diagrams based on Mach number. Since the latter is considered easier as well as more often used in the business, it is this method this thesis will proceed with.

Mach number is defined as a ratio of a velocity and the local speed of sound as in Equation 2.8 according to Çengel and Boles [6, p.780]. Using this, the velocity diagrams can be expressed based on Mach number as seen in Figure 2.5.

$$Ma_v = \frac{v}{\sqrt{\gamma R T}} \tag{2.8}$$

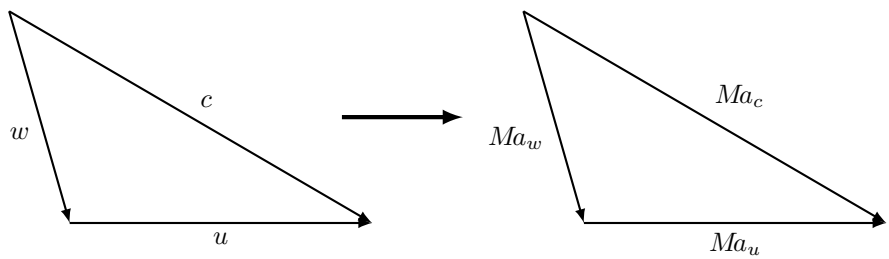

Figure 2.5. Expressing velocity diagram based on Mach number.

To calculate the Mach numbers illustrated in Figure 2.5, Ma_c, Ma_w and Ma_u, a method of examining the mass flow, rotational speed and pressure ratio described by Jonshagen [10] is used.

2.3.1 Mass flow

The mass flow through a machine is described by the equation of mass flow rate.

$$\dot{m} = \rho\, A\, c_x \tag{2.9}$$

Applying Equation 2.8 based on the axial velocity the expression of mass flow is rewritten.

$$\dot{m} = \rho\, \frac{\pi}{4}\, D^2\, Ma_x \sqrt{\gamma R T} \tag{2.10}$$

Regarding the same machine, in other words a fixed geometry, the diameter and other constants can be excluded. This combined with the ideal gas law, $p = \rho\, R\, T$, results in Equation 2.10 rewritten as Ma_x.

$$Ma_x = \frac{\dot{m}\sqrt{R\, T}}{p\sqrt{\gamma}} \tag{2.11}$$

2.3.2 Rotational speed

The blade speed, u, of a machine is described either by standard geometry or by rewriting Equation 2.8 based on blade speed.

$$u = N D\, \pi \tag{2.12a}$$

$$u = Ma_u \sqrt{\gamma R T} \tag{2.12b}$$

Combining the expressions for blade speed while excluding constants due to a fixed geometry results in an expression of Ma_u.

$$Ma_u = \frac{N}{\sqrt{\gamma R T}} \tag{2.13}$$

2.3.3 Pressure ratio

Euler's pump and turbine equation is expressed according to Dixon [11].

$$u\, \Delta c_\theta = \Delta h_0 \tag{2.14}$$

Applying Equation 2.8 based on u and c_θ respectively, Equation 2.14 results in an expression of Ma_u and Ma_θ which is further rewritten by applying the polytropic relation.

$$Ma_u\, Ma_\theta = \frac{\Delta h_0}{\gamma R T} = \frac{\eta_s \left(\pi^{\frac{\gamma - 1}{\gamma}} - 1 \right)}{\gamma - 1} \tag{2.15}$$

2.3.4 Characteristics

Using the derived Mach numbers, all Mach numbers are known according to Figure 2.6. Consequently, the velocity diagram is resolved. In other words, the gas turbine's behavior is fully described.

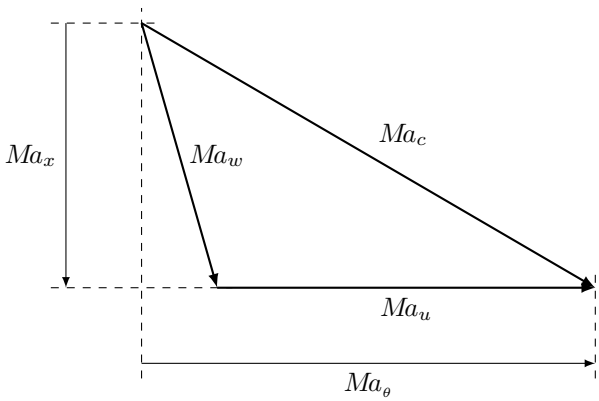

Figure 2.6. Velocity diagram based on Mach number.

To clearly visualize the performance of a gas turbine specific component characteristics are created. These characteristics, also known as compressor and turbine maps, are made from plotting the dimensionless parameter groups, that is the derived Mach numbers, to indicate the components performance in all operating conditions. It should be noted that at SIT the pressure ratio itself is used instead of the corrected pressure ratio derived in Equation 2.15. In these maps each point represents a unique velocity diagram based on Mach number and thus describes a unique operating case. The maps themselves are also unique for each component and its associated design and reveals the performance of the component in detail. For this reason, the maps are handled with great confidentiality by the companies in the industry.

Schematic illustrations of compressor and turbine maps are presented in Figure 2.7 and 2.8. In the compressor map the surge line is marked. An operating point above this line means the flow is unstable and can separate due to high positive incidence according to Razak [12]. This can in turn lead to an abrupt reversal of the flow through the compressor, potentially damaging the components. To assure a stable compression a surge margin is introduced. This safety margin defines the distance between the operating point and the surge line. To illustrate a machines operating range a running line is commonly introduced. This is a line connecting all steady state operating points at certain conditions. Additional information typically presented in compressor maps are lines of constant corrected speed and islands representing constant isentropic efficiency.

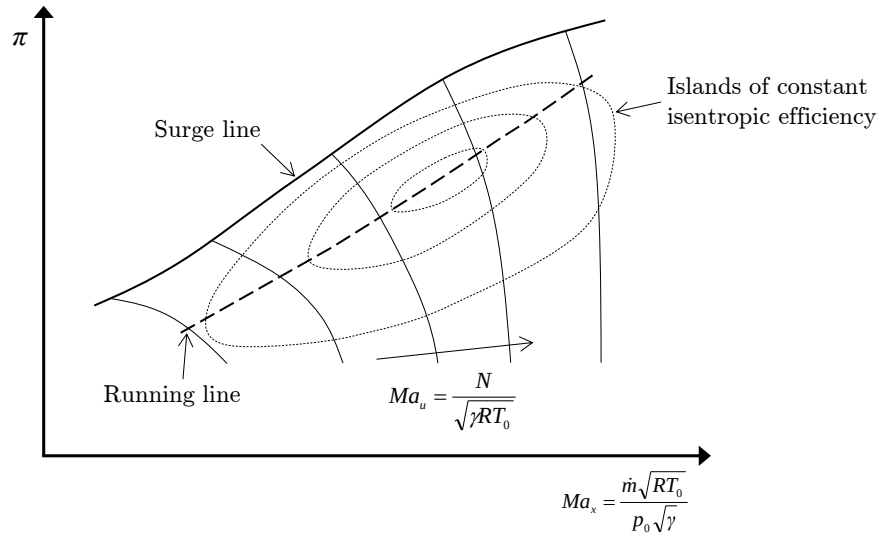

Figure 2.7. Schematic illustration of a compressor map.

Regarding turbine maps a difference is made between the cases if choking occurs in the stator or the first rotor. Noticeable about turbine maps is that the flow capacity is constant, in other words the flow is choked, throughout a wide range of pressure ratio.

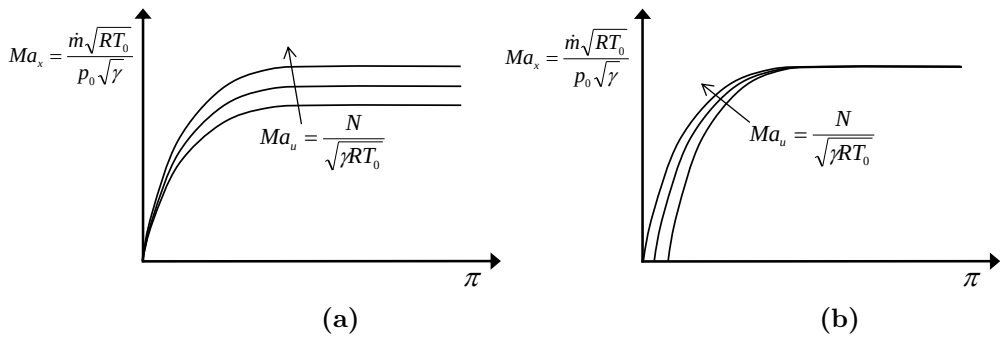

Figure 2.8. Schematic illustrations of turbine maps where choke occurs in the stator (a) or in the first rotor (b).

2.3.5 Corrected parameters

A machine's performance while running at ambient conditions deviating from ISO conditions is hard to interpret. To make it possible to compare a machine's performance regardless of its running conditions so called corrected or referred parameters are formed to reduce the number of depending variables further. This is done by correcting the parameters with reference values of certain variables as for exemple γ and R. The corrected parameters most often used in compressor calculations are corrected shaft speed and mass flow.

$$\frac{N_{corr}}{\sqrt{\gamma_{ref} R_{ref} T_{ref}}} = \frac{N}{\sqrt{\gamma R T}} \quad \Leftrightarrow \quad N_{corr} = \frac{N}{\sqrt{\frac{\gamma}{\gamma_{ref}} \frac{R}{R_{ref}} \frac{T}{T_{ref}}}} \tag{2.16a}$$

$$\frac{\dot{m}_{corr}\sqrt{T_{ref}}}{p_{ref}} \sqrt{\frac{R_{ref}}{\gamma_{ref}}} = \frac{\dot{m}\sqrt{T}}{p} \sqrt{\frac{R}{\gamma}} \quad \Leftrightarrow \quad \dot{m}_{corr} = \frac{\dot{m}\sqrt{\frac{T}{T_{ref}}}}{\frac{p}{p_{ref}}} \sqrt{\frac{\gamma_{ref}}{\gamma} \frac{R}{R_{ref}}} \tag{2.16b}$$

Having a reference temperature for a turbine is inconvenient as the full load TIT may vary due to fuel specification and differs for different versions of the machine. The corrected parameters however can be formed in any manner, what matters is that the method is consistent throughout the calculation process. Examples of custom parameters used at SIT are aero speed and flow capacity. These are variations of the corrected shaft speed and mass flow in Equation 2.16a and 2.16b respectively. It should be noted that these parameters are based on the inlet values before the cooling air is mixed into the flow, in example TIT is T_{1500} and not T_{1520}.

$$AS_{corr} = \frac{N}{\sqrt{\frac{\gamma}{\gamma_{ref}} \frac{R}{R_{ref}} T}} \tag{2.17a}$$

$$CT_{corr} = \frac{\dot{m}\sqrt{T}}{p} \sqrt{\frac{\gamma_{ref}}{\gamma} \frac{R}{R_{ref}}} \tag{2.17b}$$

2.4 Exhaust gas recirculation

Emissions at part load on twin shaft gas turbines is a well known issue discussed, amongst others, by Razak [12]. Reduction of the load is achieved by reducing the supply of fuel. Reduction of fuel mass flow affects the firing temperature which results in altered emissions according to Razak [12] as seen in Figure 2.9. Due to this phenomenon it is important to keep the firing temperature at a high level despite the load change, a state which is possible to achieve with EGR.

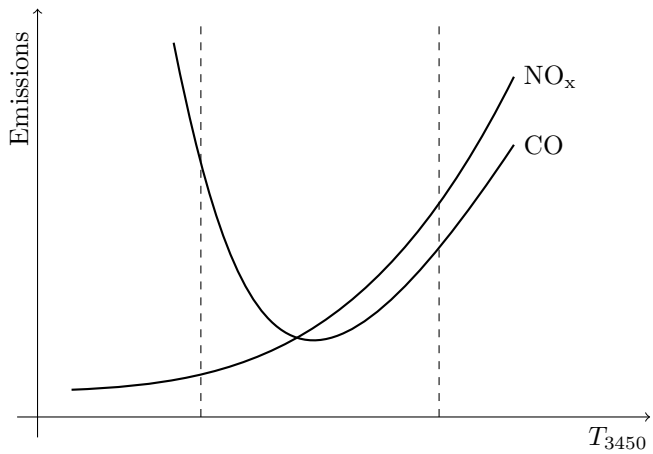

Figure 2.9. Emissions as a function of flame temperature.

The basic principle of EGR, or FGR as it is also referred to, is that a portion of the hot exhaust gases are separated from the exhaust of the gas turbine and led to the inlet where it is mixed with the colder intake air. Through this procedure the inlet air temperature is raised and hence, the inlet density reduced. This in turn results in a lower mass flow for a constant volume flow. Starting from a fixed power output the fuel mass flow is constant. This, combined with the lowered mass flow through the machine, increases the fuel to air ratio pursuant to Equation 2.18. As a result, the firing temperature is increased due to EGR. Similarly, the firing temperature can be kept constant as the power output decreases due to EGR.

$$FAR = \frac{\dot{m}_{fuel}}{\dot{m}_{air}} \tag{2.18}$$

To measure and express EGR as a ratio is an applicable method. However, the definition of the term differs from work to work. In this thesis EGR is defined as the ratio of the recirculated mass flow and the exhaust mass flow before EGR extraction.

$$EGR = \frac{\dot{m}_{EGR}}{\dot{m}_{0850}} \tag{2.19}$$

2.4.1 Additional positive effects of EGR

Aside from keeping the firing temperature high with lowered load, the purpose of EGR in this thesis, the method also offers several other benefits. If the hot exhaust gases are mixed with the intake air before the intake air filter, the hot recirculation works as a free anti icing system. Thus, a separate system to deal with icing of the intake air filter will not be needed, a system that would increase losses.

Another advantage of implementing EGR in the gas turbine cycle is that the concentration of CO_2 is increased. This in turn significantly decreases the energy demand of CCS as shown by Li *et al.* [13].

2.4.2 Limitations of EGR

Temperature limitations
To reduce weight, and also simplify the manufacturing process and hence the costs, the inlet casing of the SGT-750 is made of a composite material, Tageman [4]. Nilsson [14] establishes that with the material used today, this implies a temperature limit of 90 °C at continuous load while a higher temperature, 130 °C, is allowed instantaneous. Since the purpose of EGR is to increase the inlet temperature, this is an unquestionable limitation. However, in the case of an inlet temperature rise above an acceptable level other composite materials such as Vinyl Ester can be used, Nilsson [14]. In this case the temperature limit increases to approximately 160 – 200 °C.

An increase in compressor inlet temperature also results in a temperature rise further down the compressor. Eventually a temperature is reached when the flow is to hot to work as necessary cooling flow. The problem is examined by Andersson [15], resulting in a limit in the compressor outlet temperature.

The positive side effect of an EGR system that works as a free anti icing system also has its limitations. Jonsson [16] states that todays solution of handling ventilation to the SGT-750 enclosure is to use the same intake air filter as to the machine itself. This problem is however easy to solve with a rather simple construction modification. Furthermore, the intake filter itself is limited in temperature, according to Jonsson [16] at 80 °C locally for hot strings if the flow is inhomogeneously mixed and at 70 °C in general. A possible solution to this problem is to mix the hot exhaust gases with the intake air after the filter, but the advantage of a free anti icing system is then lost. Also, this solution would have a negative impact on the efforts to achieve an as clean as possible environment after the intake air filter. This effort is, according to Tageman [4], made to minimize the risk of getting unwanted items, such as metal objects, in the system that may be harmful to the compressor.

Oxygen limitations

With increasing EGR the oxygen content is decreasing in the combustion chamber outlet. A lack of oxygen results in incomplete combustion, an undesirable state, which limits the percentage of EGR possible to fulfill. According to Janczewski [17] a minimum oxygen content of 8 % in the combustion chamber outlet is required to ensure complete combustion.

Lifing

Lifing of gas turbines are greatly related to rotational speed since centrifugal tensile stress of the blades relates to rotational speed according to Equation 2.20, Cohen *et al.* [2, p.298]. This implies that possible variations in rotational speed due to variation in load are important. There is a limit of 9400 rpm for the SGT-750, according to Tageman [4]. However, it should be borne in mind that an increased speed always implicates a decrease in lifetime of a gas turbine.

$$\sigma \propto AN^2 \tag{2.20}$$

Further example of a factor affecting the lifing of gas turbines is the TIT. A higher temperature results in a shortage of lifespan for the machine according to Jonshagen [18].

2.4.3 Practical aspects of implementing EGR

When implementing EGR in the gas turbine cycle some practical aspects has to be taken into account. The flow has to be extracted from the exhaust at a convenient location. It has to be led through piping of sufficient dimensions and be pressurized by a fan. This fan can also, in some cases, serve as a component to mix the intake air with the hot exhaust gases to guarantee a good temperature distribution of the flow. Finally the flow has to be inserted back into the cycle.

2.5 IPSEpro and the Newton-Raphson method

IPSEpro, a software developed by SimTech Simulation Technology, is a heat and mass balance calculation program. It is a matrix solver that puts all equations of a system in a matrix. To speed up the calculating process, the program at first divides the matrix into sub matrixes to separate non depending variables from each other. After this, the equations in each submatrix are solved simultaneously with the Newton-Raphson method.

2.5.1 IPSEpro

The working principle of IPSEpro is that the model built is composed of components containing the heat and mass balance equations necessary for equilibrium. The components and its equations are accessible in the complementary software MDK. MDK is a software used to view and modify existing equations, but also to add variables and equations into existing components or creating brand new components. MDK stores the components in so-called library files. With the software SimTech provides a standard library of power plant components called *advanced power plant library* or *applib*.

In IPSEpro the tolerances and iteration parameters are set in the software settings. These settings works as criteria for convergence of the calculations. To carry out a full calculation, the correct number of parameters in relation to the number of existing equations in MDK also has to be set. The software then solves the equation system according to the Newthon-Raphson method.

2.5.2 The Newton-Raphson method

The basic principle of the Newton-Raphson method is that it, on the basis of a starting estimate, finds better and better approximations to the roots of a function on the form of $f(x) = 0$. As the iteration continues the approximations converges and a solution is obtained. This method is a fast way to solve a large number of equations although it lacks in reliability because of the risk of calculating the wrong or no roots with poor initial estimates. The method can mathematically be described as follows, with notations according to Figure 2.10.

By starting with the estimate x_n, $f(x_n)$ is calculated and $f(x)$ is estimated locally with its linear tangent $g(x)$ given by the point slope formula described by Böiers and Persson [19, p.25].

$$g(x) = f'(x_n)(x - x_n) + f(x_n) \tag{2.21}$$

The intersection between the function $g(x)$ and the x axis, referred to as x_{n+1}, is generally a better estimation to the root of $f(x)$.

$$x_{n+1} = x_n - \frac{f(x_n)}{f'(x_n)} \tag{2.22}$$

This procedure is repeated by IPSEpro until the error, $|x_{n+1} - x_n|$, is below the given tolerance, in other words when the solution has converged.

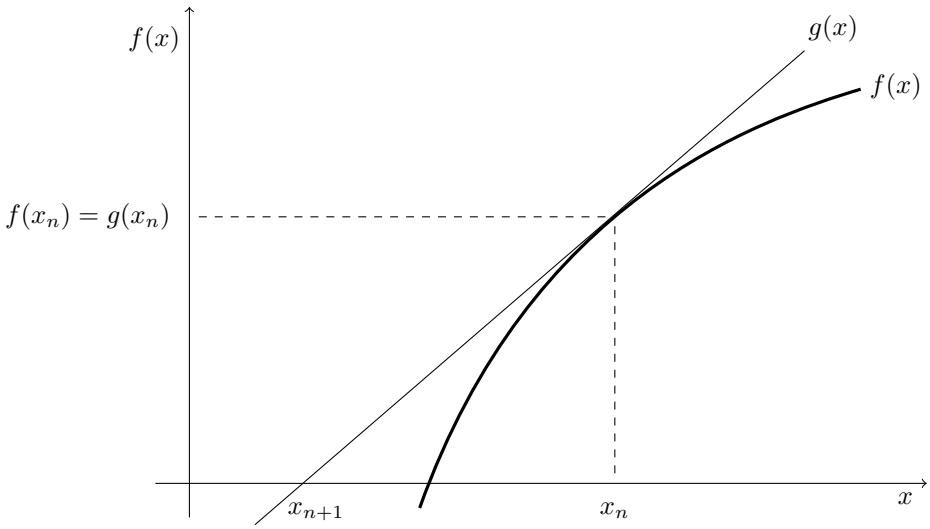

Figure 2.10. Illustration of the Newton-Raphson method with notations.

3

Methodology

The general approach to fulfill the purpose of this thesis was to create a standard model of the gas turbines examined. The model was constructed to automatically read Siemens component characteristics to ensure its validity. Furthermore, the model was validated against Siemens performance programs to ensure its correspondence with reality. A model that was consistent with the performance programs was able to give a useful indication of how the gas turbine would behave under changing circumstances. The model was thereafter complemented with EGR and its impact and potential was examined as a method to improve the gas turbine's performance and emissions at part load.

3.1 Software selection

The software used in the work process were naturally selected. IPSEpro was selected to create the model since it is the standard software to perform model calculations at SIT's department of research and development. Due to the same reason, the program selected to validate the model's calculations was the SIT intern performance calculation program, GTPerform. The work with developing a DLL file was conducted in Microsoft Visual Studio 2010, with C++ as programming language. This choice was made mainly because earlier work of creating executive files, with the purpose of making IPSEpro communicate with text files, using this software and language has been carried out at the Department of Energy Sciences by Mondejar [20].

3.2 Development of DLL file

To get IPSEpro to load data from Siemens text files of component characteristics, a DLL file was developed. DLL files provides a way for an application to call functions that are not part of its executable code and are the recommended files to implement external functions in MDK according to SimTech [21]. The technicalities and method behind creating the file is described by Mondejar [20]. A disadvantage of using DLL files to communicate with IPSEpro is that error messages occurring when executing the file are difficult to handle. The option of passing error messages from the DLL file to IPSEpro is available in MDK but its applicability is limited.

3.2.1 Read data

A function *read* was written to read the data from the text files. The purpose of the function was to read and interpret the information from Siemens component characteristics and store it in variables. The main technical challenge of the *read* function was to make the DLL file future-proof and versatile. In example, the characters of a string was not read from character x to y on a given line but instead read from the first character not consisting of a white space to the character before next occurring white space.

3.2.2 Perform calculations

The *calc* function was written to perform the calculations. It calculates the mass flow and efficiency based on the input data of corrected shaft speed and pressure ratio by interpolating in the characteristics. Specific parameters were built in the calculations to control whether the input parameters were within the boundaries of the characteristics. If not, the calculations returned excessive results to IPSEpro to force a change in derivative and thus, a changed input in the next iteration of calculations.

3.2.3 Main functions and derivatives

The necessary functions to get the DLL file to interact with IPSEpro were created. These consisted of one main function and two derivatives for each return value. The derivatives were numerically calculated using the definition of the derivative according to Böiers and Persson [19, p.187].

$$f'(x) = \lim_{x \to 0} \frac{f(x+h) - f(x)}{h} \tag{3.1}$$

3.2.4 Description of the code

An extract of the actual code written, the preamble and functions related to the compressor, is presented in the Appendix A whereas a more general description of the code's cornerstones is presented in sequential order below.

- Initially some basic libraries are included.
- The necessary functions for a DLL file to communicate with IPSEpro are included according to the manual by Mondejar [20].
- Some miscellaneous objects as vectors and other variables are defined.
- The function *read*:
  - After the input data file is opened a while loop traverses and reads all the lines of the file.
  - After commentary lines are skipped some miscellaneous values as for example the number of IGV angles and number of speed lines are read.
  - The code continues with looping all speed lines and for each speed line traversing and reading its included lines of values. In the case of the compressor these values are the corrected mass flow, pressure ratio and polytropic efficiency while they for the turbines are flow capacity, pressure ratio and isentropic efficiency.
  - The input data file is closed.
- The function *calc*:
  - The speed lines are traversed to find the two speed lines relevant to interpolate between with regard to the input data of speed.
  - For each of the two speed lines, its corresponding table of pressure ratio is traversed to find the two pressure ratios relevant to interpolate between with regard to the input data of pressure ratio.
  - With linear interpolation the return values are calculated. These are mass flow and polytropic efficiency for the compressor and flow capacity and isentropic efficiency for the turbines. If the input data is outside of the characteristics, the function returns a mass flow or flow capacity of zero and an efficiency of 100 % to force IPSEpro to change its derivatives, as described in Section 3.2.2.
  - In the case of the power turbine an extra input data of turbine match is used to determine which characteristics to use.
- External functions and associated derivatives are included.

3.3 Construction of model

Initially a model was put together using standard components from *applib*. The working procedure was to start from a basic model of a gas turbine and complement it with more advanced components as the work progressed. This resulted in a new library containing all modified components and equations. Throughout the process, the work was performed with a general mindset to make the model durable and increase its interchangeability for future possible changes of the gas turbine configuration.

The SIT specific theory and nomenclature used in the process of modeling the components is described in the *SIT Performance Model* by Sjödin [22].

3.3.1 SAS

Construction of the secondary air system started with examining the gas turbine's reference file. This file states from where and at what temperature and enthalpy ratio in the compressor the cooling flows are extracted, and at what location in the process they are inserted again. With this information the necessary splitters and mixers could be modeled.

The biggest effort put into this part of modeling was with creating the necessary splitters for the cooling flows, Figure 3.1a. To facilitate future development of models of other gas turbines in the company, they were made general. Every splitter was created with three, and in some cases four, output ports. When adding the splitter to the model, every port's destination was selected in a drop down list as presented in Figure 3.1b, for example 0850, leak or no connection. These choices made the correct splitter fraction to be obtained from the global object containing all fractions from the gas turbine reference file.

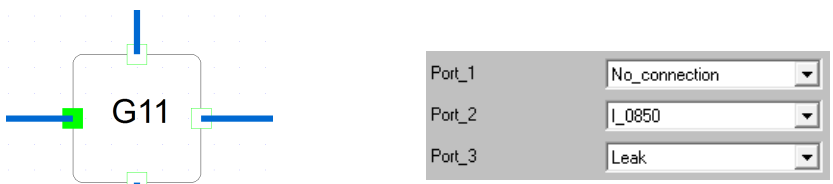

(a) Cooling flow splitter. **(b)** Port settings.

Figure 3.1. Secondary air system splitter with settings.

3.3.2 Modeling with characteristics

The characteristics describes, as mentioned in Section 2.3.4, a components performance and behavior in all operating conditions. The general approach when modeling with characteristics is to set a reference point to which all other parameters can be related. In this case it was done by setting the reference values as input data in the components in IPSEpro.

The relation between the actual, relative and reference values of a variable was calculated as follows. However, the pressure ratio was calculated differently to ensure a pressure ratio of one when no pressure rise or drop occurs, in accordance with Sjödin [22].

$$X_{rel} = \frac{X}{X_{ref}} \tag{3.2a}$$

$$\pi_{rel} = \frac{\pi - 1}{\pi_{ref} - 1} \tag{3.2b}$$

3.3.3 Compressor

With set reference values, the corrected parameters were calculated according to Equation 2.16a and 2.16b and with Equation 3.2a and 3.2b, the relative parameters were calculated. After this, functions were created in MDK to communicate with the DLL file and calculate the mass flow and polytropic efficiency as a function of relative speed and pressure ratio.

$$\dot{m}_{rel} = f(N_{rel}, \pi_{rel}) \tag{3.3a}$$

$$\eta_{p,rel} = f(N_{rel}, \pi_{rel}) \tag{3.3b}$$

3.3.4 Turbine

A problem regarding the turbine expansion is that it either has to start from the real turbine inlet, in the example of the compressor turbine at 1500, or from a fictitious state where all cooling air is mixed in with the flow, at 1520. Neither of the methods are correct since it, in reality, is a gradual process. This was solved by modeling the expansion from the fictitious mixed inlet state and placing probes in the model before the cooling air was mixed in. These probes were used to communicate the variable values at the location of the probe with the turbine to calculate the different parameters. This was done because if all variables used to calculate the parameters for the characteristics, for example flow capacity, were fetched at the mixed inlet, a change in cooling mass flow would not affect these parameters.

The corrected parameters were calculated according to Equation 2.17a and 2.17b, after which the relation between the corrected, relative and reference value of vari-

ables in the turbine were calculated with Equation 3.2a and 3.2b. Functions were created to calculate flow capacity and isentropic efficiency as a function of corrected aero speed, pressure ratio and matching conditions, using the DLL file created. The matching condition indicated whether the function should perform calculations using normal or tropical matching of the gas turbine. This option was however only relevant for the power turbine.

$$CT_{rel} = f(AS_{rel}, \pi_{rel}, \text{match}) \tag{3.4a}$$

$$\eta_{s,rel} = f(AS_{rel}, \pi_{rel}, \text{match}) \tag{3.4b}$$

3.3.5 Combined cycle

An additional model was created were the gas turbine, referred to as the top cycle in a combined cycle, was added an existing model of a bottoming cycle from SIT. An existing model was used since modeling this was not considered a purpose of this thesis. The bottoming cycle consisted of a dual pressure heat recovery steam generator, HRSG, using heat from the exhaust gases of the gas turbine to produce steam for a simple Rankine steam cycle.

3.4 Validation

The model's conformance with Siemens performance programs was a key criterion for the work to proceed. A number of important sections throughout the machine was examined and key values in these sections were compared against the corresponding values calculated by GTPerform. This process was performed for different operating conditions with varied ambient temperature and load. Sections were the deviation was significant were examined thoroughly in MDK and errors were corrected.

With the goal to eliminate the residual error, the main components were examined separately. With values from GTPerform set in IPSEpro as input and output data in the components, their calculations were verified. The results yielded a remaining error of the same magnitude resulting in further investigation. A single stream with the same composition, temperature and pressure as in GTPerform was examined. With a remaining error the reason was found to be a difference in gas data, the physical properties are calculated differently. IPSEpro uses JANAF, Joint Army Navy Air Force, Thermochemical Tables [23] whereas GTPerform uses NASA SP-273. The deviation was considered to be within the margin of error and the process of model validation was completed.

An issue appearing during the process of validating the compressor component separately was that the input data to the DLL file sometimes was outside the tables of characteristics. The interpolation in the function calc would not work and the model did not converge, it was instable. An idea if creating so called beta lines, slanting lines in the compressor map as input data was examined but the issue was solved automatically when connecting the compressor to the compressor turbine. The gas generator as a unit affected the quantities simultaneously and the model became stable, the running line basically worked as a beta line.

3.5 Complementing with EGR

The model was complemented with EGR in different setups depending on whether it was for the simple or combined cycle.

3.5.1 Simple cycle

In the case of the simple cycle, the model was complemented with a stream recirculating exhaust gases from the exhaust before the outlet pressure drop, at 0850, to the inlet before the intake air filter, at 0100. To drive the flow forward and manage the issue of mixing the cold inlet air and hot exhaust gases to guarantee a good temperature distribution, a fan was added to the model. This fan was powered with a motor affecting the total power produced since the motor consumes power.

The performance of the fan was set to necessary values according to Andersson [24] with a total pressure rise of 13.26 mbar over the complete section of EGR. In addition the isentropic, electrical and mechanical efficiencies of the motor were all set to 90 %. This was made to ensure a satisfying safety margin in the calculations although both the electrical and mechanical efficiency might be too restrictively set. To satisfy the demands of the fan, a maximal inlet temperature of 300 °C had to be guaranteed according to Tageman [4]. This was ensured by mixing a sufficient part of the ambient air with the recirculated exhaust gases before the fan.

3.5.2 Combined cycle

A stream recirculating the exhaust gases from after the HRSG to the gas turbine inlet before the intake air filter, at 0100, was added. To simulate the pressure drop of the HRSG, the outlet pressure drop was approximated to 25 mbar. A fan and motor, as used in the simple cycle, was necessary also in this case. However, mixing the recirculated exhaust gases with the intake air before this fan was not necessary due to the lower temperature of the gases. In addition to this, the feed water pumps in the bottoming cycle were added motors with the same specifications as the EGR fan consuming power and hence, negatively impacting the total power produced.

A variant of the combined cycle was also created with the same EGR case as for the simple cycle to be able to fully compare the two and clarify the potential of the combined cycle.

3.6 Analysis

To investigate the impact of EGR, the following cases were examined and compared with varied load for the simple cycle model. The cases are also explained with TIT as a function of load in Figure 3.2.

Case 1: Today's way of handling issues with emissions by bleeding pressurized air from the compressor outlet to the gas turbine exhaust. Method explained in detail in Section 2.1.1.

Case 2: Substituting bleed with EGR. The method is the same as Case 1 but T_{1520} is kept constant with varied load by increasing EGR from exhaust to inlet instead of bleeding.

Case 3: Keeping T_{1520} constant at the same level as at full load. Compensating load decrease with EGR from exhaust to inlet straight from the initiation of the load variation.

With an added bottoming cycle in the combined cycle model two additional cases emerged since EGR is possible from after the HRSG as well.

Case 4: Case 2 with EGR from outlet of HRSG.

Case 5: Case 3 with EGR from outlet of HRSG.

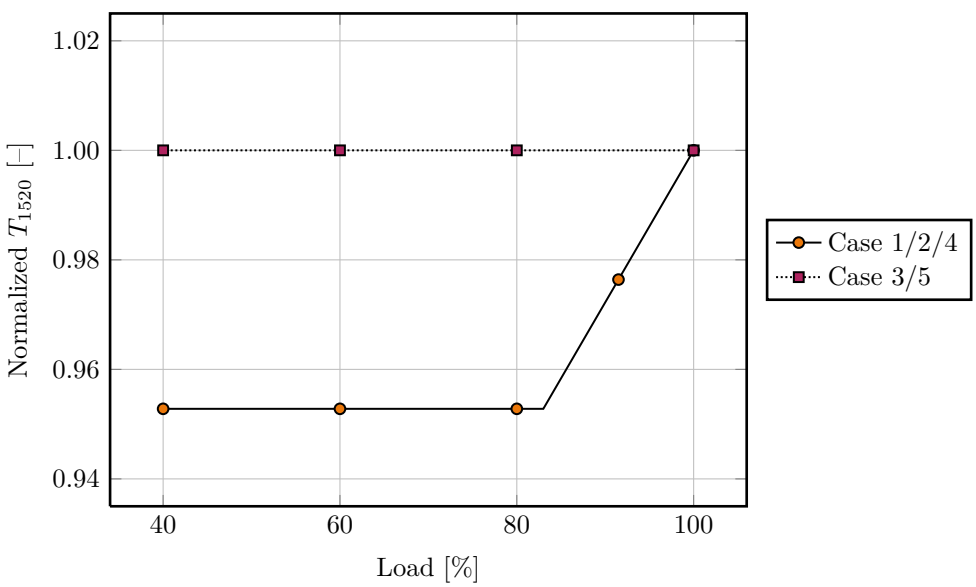

Figure 3.2. TIT as a function of load for the cases analyzed.

3.6.1 Comparision

All cases were examined with ambient temperature of 15 °C and normal turbine match of the power turbine as well as with ambient temperature of 30 °C and tropical turbine match. Significant parameters were plotted against load or other key parameters to illustrate the gas turbine's performance and behavior at part load. The differences between the cases were then analyzed based on the theory and results. Further tests were performed to either eliminate or determine certain parameter's influence on the results.

The cases were examined with decreasing load from 100 % to 40 %. In the cases with EGR from the HRSG outlet, Case 4 and 5, the combustion turned problematic with decreasing oxygen content due to increasing EGR. The requirement of oxygen content in the combustion chamber outlet was not satisfied at lower loads and the calculations could not be performed all the way down to 40 %.

To make the comparison fair and make the cases similar T_{1520} was allowed to be reduced to the same level in Case 1, 2 and 4. As mentioned in Section 2.1.1, in the case of bleeding, T_{1520} is allowed to be lowered further after a specific bleed mass fraction is reached. This would have had a positive effect on the performance while affecting emissions negatively and allowing it in the comparison would be like comparing apples and oranges and was therefore considered irrelevant.

It should be borne in mind throughout the analysis that the SGT-750 is not actually designed and optimized to work in a combined cycle. The exhaust gas temperature at ISO conditions is relatively low, 459 °C [3], resulting in poor performance of the bottoming cycle.

3.6.2 Practical analysis

The practical implementation of EGR was analyzed by calculating the needed diameter of the pipes to satisfy different pressure losses with the equations described in Section 2.2.3. This was done using goal seek, a numeric approximation method. By iteration different diameters were used to try to satisfy given pressure losses, in this case a pressure loss of 13.26 mbar in accordance with Andersson [24] and 0.1 bar as an arbitrary estimate. The lower of these losses was chosen because the calculations throughout this thesis are based on this pressure loss as described in Section 3.5.1 while the latter was examined because a higher accepted pressure loss would result in a reduced diameter.

The assumptions made for the pipe loss calculations are presented below. The values are assumed with conditions after the EGR fan since it is physically located close to the extraction point and most of the recirculation actually occurs after this fan.

- The pipe length is assumed to be 10 m for the simple cycle and 15 m for the combined cycle since the distance is further in this case.
- Equivalent roughness is approximated as the roughness for commercial steel, 0.045 mm [7, table 8.1].
- The dynamic viscosity of air at 300 °C is used, $2.98 \cdot 10^{-5}$ Pa s [7, table B.4]. This is since the combustion is made with excess oxygen resulting in nitrogen gas as the dominant element of the flue gases as is the case with ambient air. The dynamic viscosity is independent of pressure.
- For the simple cycle the mass flow and density at 50 % load are used while for the combined cycle the values related to an oxygen content of 8 %, resulting in a load of 62.134 %, are used.
- The loss coefficient was estimated with four long radius 90° flanged bends and one gate valve ¼ closed resulting in a total loss coefficient of 1.06.

As the greater of the two pressure drops examined would have had negative influence on the performance, the power consumed by the fan and the cycle efficiency were calculated to assure a change within the limits of what is considered acceptable.

The material needed for a safe recirculation was determined to be 16Mo3 in collaboration with Lindman [25] with reference to a conducted project regarding anti icing piping. This steel is, according to one supplier, able to withstand wall temperatures of approximately 530 °C [26].

4

Results

The standard model of the SGT-750 created in IPSEpro as a part of this thesis is based on the gas turbine's characteristics which cannot be made public. However, an illustration of the model is presented in Figure 4.1. The process also resulted in models with EGR instead of bleed, used for further work in this thesis. All models are relatively general in their execution and therefore future proof for further work and development. This will also facilitate any adjustments to construct models in IPSEpro of other gas turbines in the company's product portfolio.

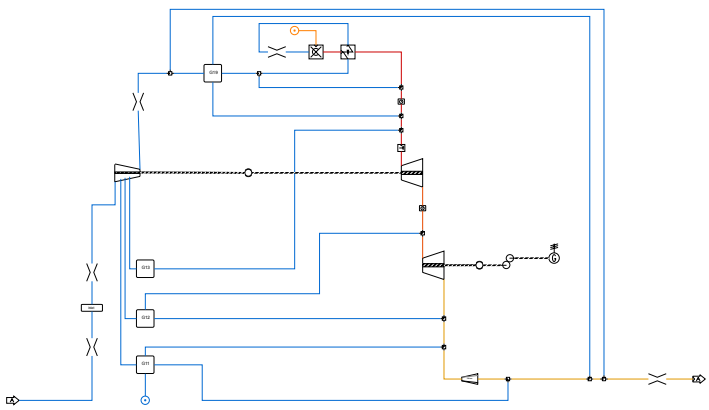

Figure 4.1. Standard model of the SGT-750 with bleed.

4.1 Validation of model

The process of model validation resulted in an average deviation in the range of 0.05 – 0.1 % depending on ambient and load conditions. The residual error is determined to be caused by errors in enthalpy calculation due to differences in gas data. A subset of the comparison is presented in Table 4.1, while the full comparison is presented in Table B.1, Appendix B.

Table 4.1. Subset of comparison of results from model in IPSEpro and GTPerform.

	ISO conditions	T_{amb} 45 °C	T_{amb} -25 °C	P_{gen} 22 MW
1200				
p	0.00 %	0.00 %	0.00 %	0.00 %
T	0.00 %	0.00 %	0.00 %	0.00 %
h	0.09 %	0.09 %	0.31 %	0.09 %
$\dot{m}$	0.08 %	0.18 %	0.01 %	0.01 %
Generator 00				
P	0.20 %	0.40 %	0.00 %	0.00 %
P_{loss}	0.16 %	0.18 %	0.00 %	0.00 %
Average	**0.057 %**	**0.098 %**	**0.063 %**	**0.045 %**

4.2 Simple cycle

The result of comparing the three cases studied will be presented through plotting and examining relevant parameters' variation with load. As mentioned in Section 3.6, Case 1 is using bleed, Case 2 is lowering the mixed TIT to the same level as with bleed while in Case 3 it is kept high throughout the load variation. It should be noted that some results are normalized due to confidentiality.

4.2.1 EGR

The percentage of recirculated mass flow, the definition of EGR in this thesis, is increasing with lowered load. An in principle linear behavior is seen when examining EGR as a function of load resulting in a recirculation with ISO conditions and normal match in the range of 7 – 9 % on 50 % load depending on the case studied as seen in Figure 4.2. The same overall behavior is found when the gas turbine is tropically matched.

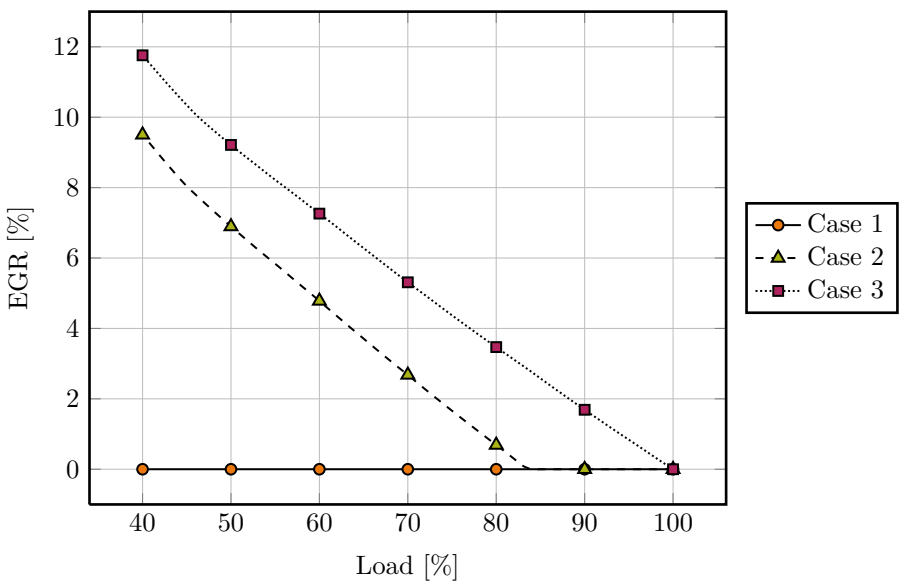

Figure 4.2. EGR as a function of load for normal match.

4.2.2 Cycle efficiency and pressure ratio

It is found that the cycle efficiency increases significantly with EGR in relation to bleed as presented in Figure 4.3. The reason is that when bleeding, a noticeable portion of pressurized air is dumped to the exhaust. Air that has been added work by the compressor but is not utilized in the process. A difference in cycle efficiency is also observed in the comparison between the different cases of EGR, Case 2 and 3. This relates to the difference in pressure ratio presented in Figure 4.4 since Equation 2.4 states that efficiency is a function of pressure ratio.

In Figure 4.4 a difference in pressure ratio cannot be spotted between Case 1 and 2 although the data yields a minor deviation. The cases differs slightly in heat input due to the difference in cycle efficiency. This small difference multiplied with a fuel to air ratio in the range of two percent results in a basically equal pressure ratio in the two cases.

The pressure ratio is also examined and presented as a compressor working line in Figure 4.5. It reveals a running line in Case 2 and 3 closer to the surge line than in Case 1. Despite the fact that the cases of EGR results in a higher efficiency, problems regarding stability must be considered. When running a gas turbine, a safety margin to surge is necessary to manage changing conditions as for example rapid load ramp up. That being said, these results does not disclose the surge margin.

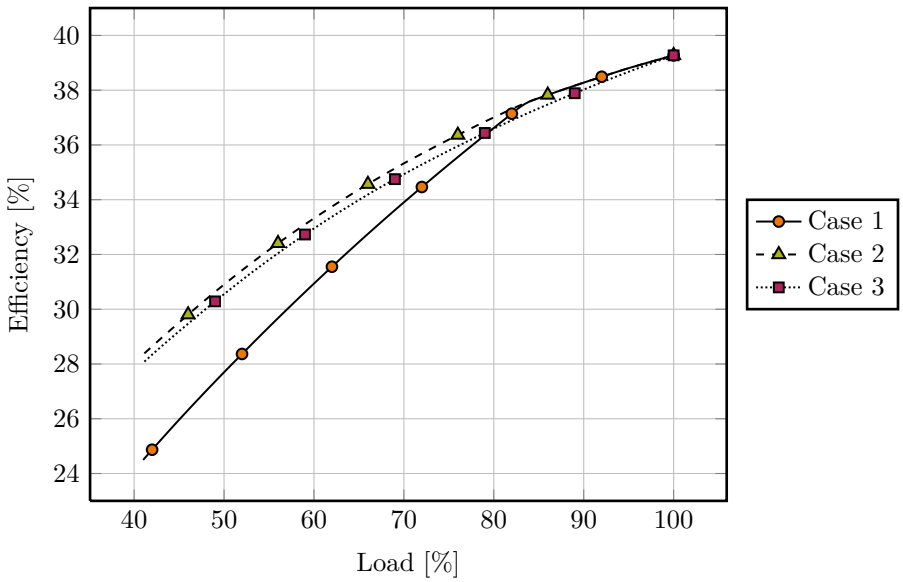

(a) Normal match

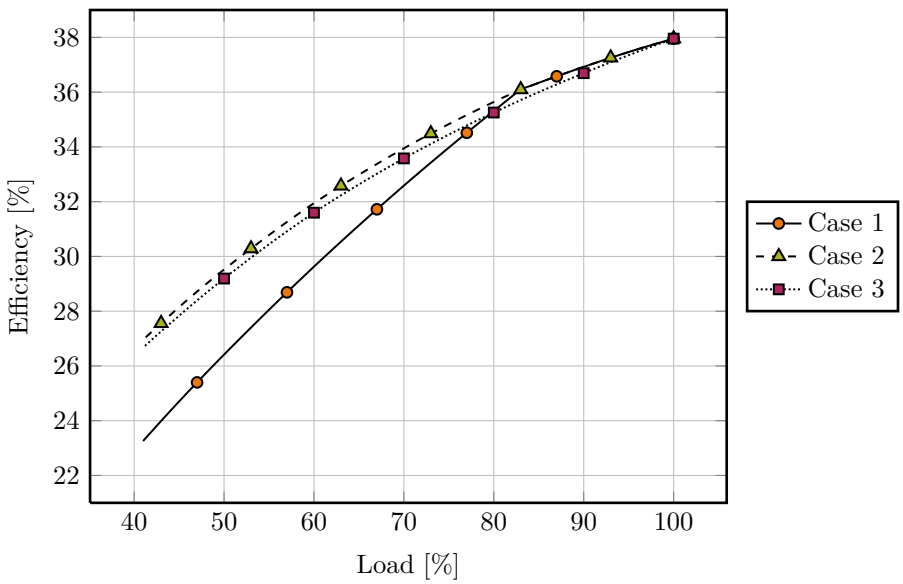

(b) Tropical match

Figure 4.3. Cycle efficiency as a function of load.

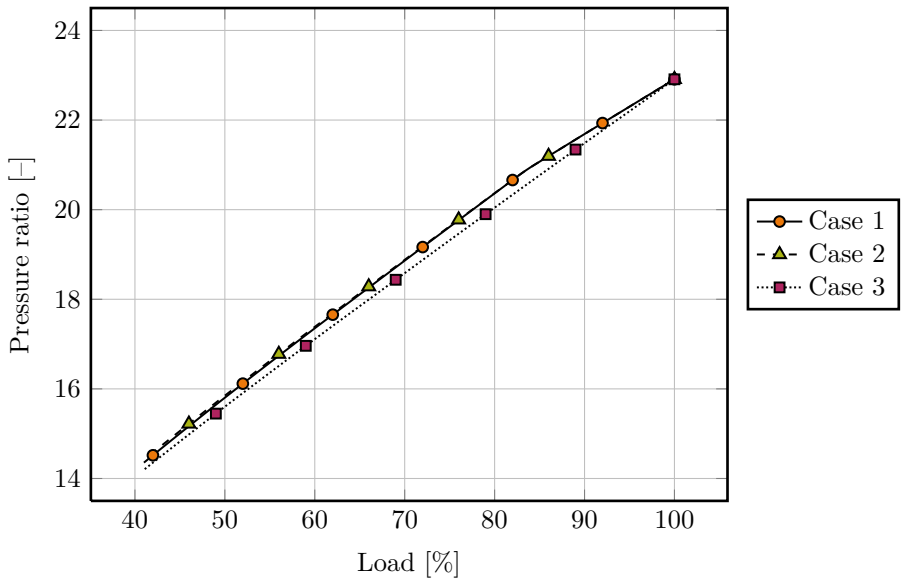

Figure 4.4. Compressor pressure ratio as a function of load for normal match. The same behavior is found when the gas turbine is tropically matched.

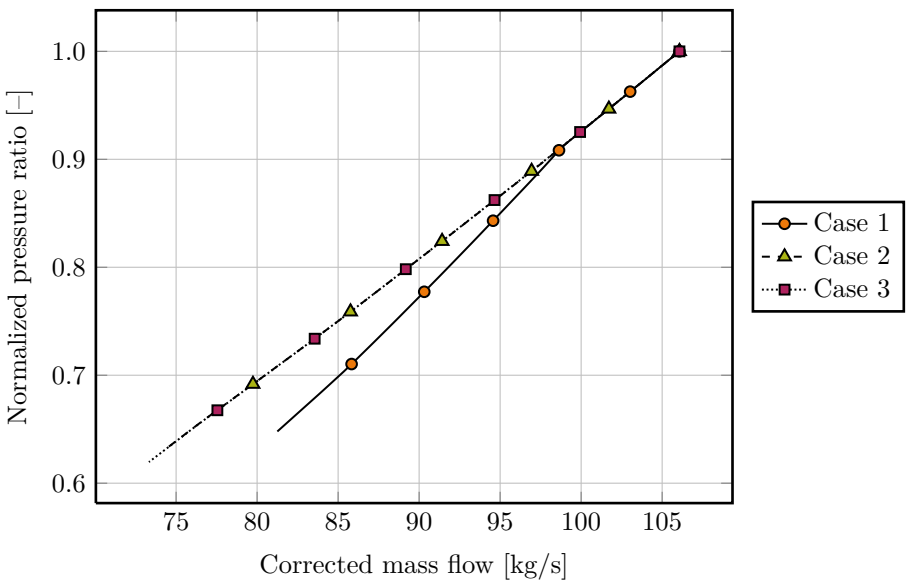

Figure 4.5. Compressor working line for normal match. The same behavior is found when the gas turbine is tropically matched.

4.2.3 Component efficiencies

The compressor polytropic efficiency varies only slightly between the three cases studied, as seen in Figure 4.6. The increased compressor inlet temperature leads to an operating point further from the design point and hence, a decrease in compressor efficiency.

To illustrate that the overall results are only vaguely related to the component efficiencies, the compressor polytropic efficiency, with reference to Section 2.2.2, was set constant which revealed close to no change in cycle efficiency. The turbine efficiencies does not either vary appreciably. In conclusion, the variation in component efficiencies due to EGR is found to have very little influence on the overall cycle.

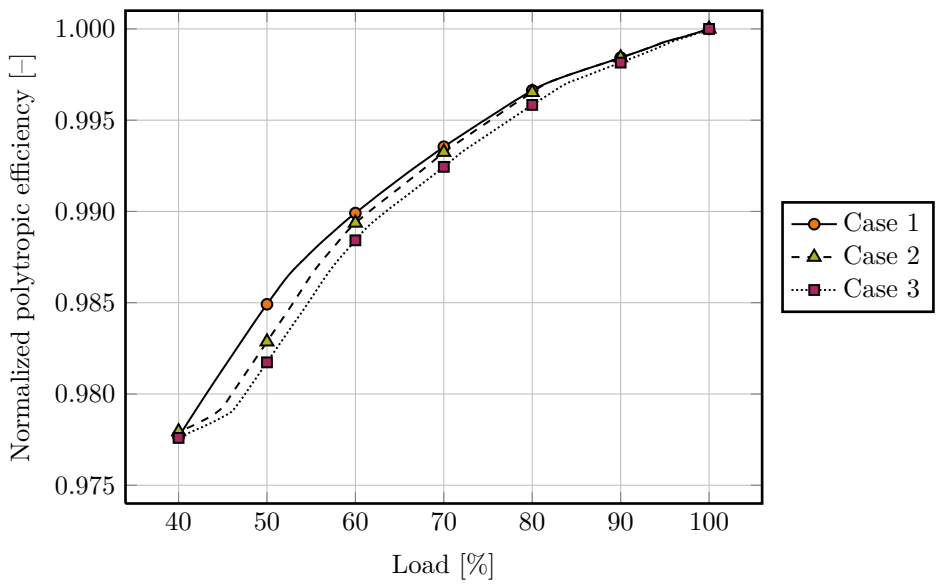

Figure 4.6. Compressor polytropic efficiency as a function of load for normal match. The same behavior is found when the gas turbine is tropically matched.

4.2.4 Compressor temperatures

The compressor temperatures varies with load according to Figure 4.7. The limit of compressor inlet temperature at 90 °C is reached in Case 3 with tropical matching of the power turbine. As mentioned in Section 2.4.2 this limit is not set in stone and the compressor inlet can handle higher temperatures momentarily. That being said, the temperature limit in the compressor outlet is also reached in this case.

Furthermore, if the EGR is used as an anti icing system and the hot exhaust gases are mixed with the ambient air before the intake air filter the general temperature limit of 70 °C applies. However, there is a workaround of this problem as discussed in Section 2.4.2 of not using EGR as an anti icing system.

4.2.5 Shaft speed

The physical rotational speed is an important parameter in aspects of solid mechanics and lifing. The results presented in Figure 4.8a and 4.8b yield that with increasing rate of EGR due to lowered load the physical shaft speed increases, while it decreases with bleed. The behavior of Case 2 is especially noticed to at first decrease in shaft speed then, when EGR is initiated, increase again. The downward trend of shaft speed due to bleed can be explained by a lower mass flow through the turbine. This results in a decrease in pressure due to a relatively constant flow capacity according to Equation 2.17b. A lower pressure build-up in turn leads to lower shaft speed.

The upward trend of shaft speed due to EGR is a consequence of the fact that more work has to be performed to compress the heated inlet air. The compressor compensates this with an increase in mass flow, in other words an increased shaft speed. Worth noticing is that in Case 3 the rotational speed limit of 9400 rpm is reached at approximately 60 % load and tropical match, a limit not acceptable to exceed. Also, studying the corrected compressor speed in Figure 4.8c and 4.8d reveals a decrease in all shaft speeds when corrected for temperature and gas properties.

While physical shaft speed is of importance in terms of mechanical aspects, the turbine aero speed is the parameter perceived by the flow affecting the aerodynamic performance in general. The aero speeds presented in Figure 4.9a and 4.9b shows an increase in all cases except for Case 1 after the bleed valve is opened. When bleed is initiated a rapid change occurs and the aero speed is decreasing. This behavior is consistent and impacts for example the cycle efficiency as seen in Figure 4.3 where a sudden change in gradient for Case 1 is found at just over 80 percent load.

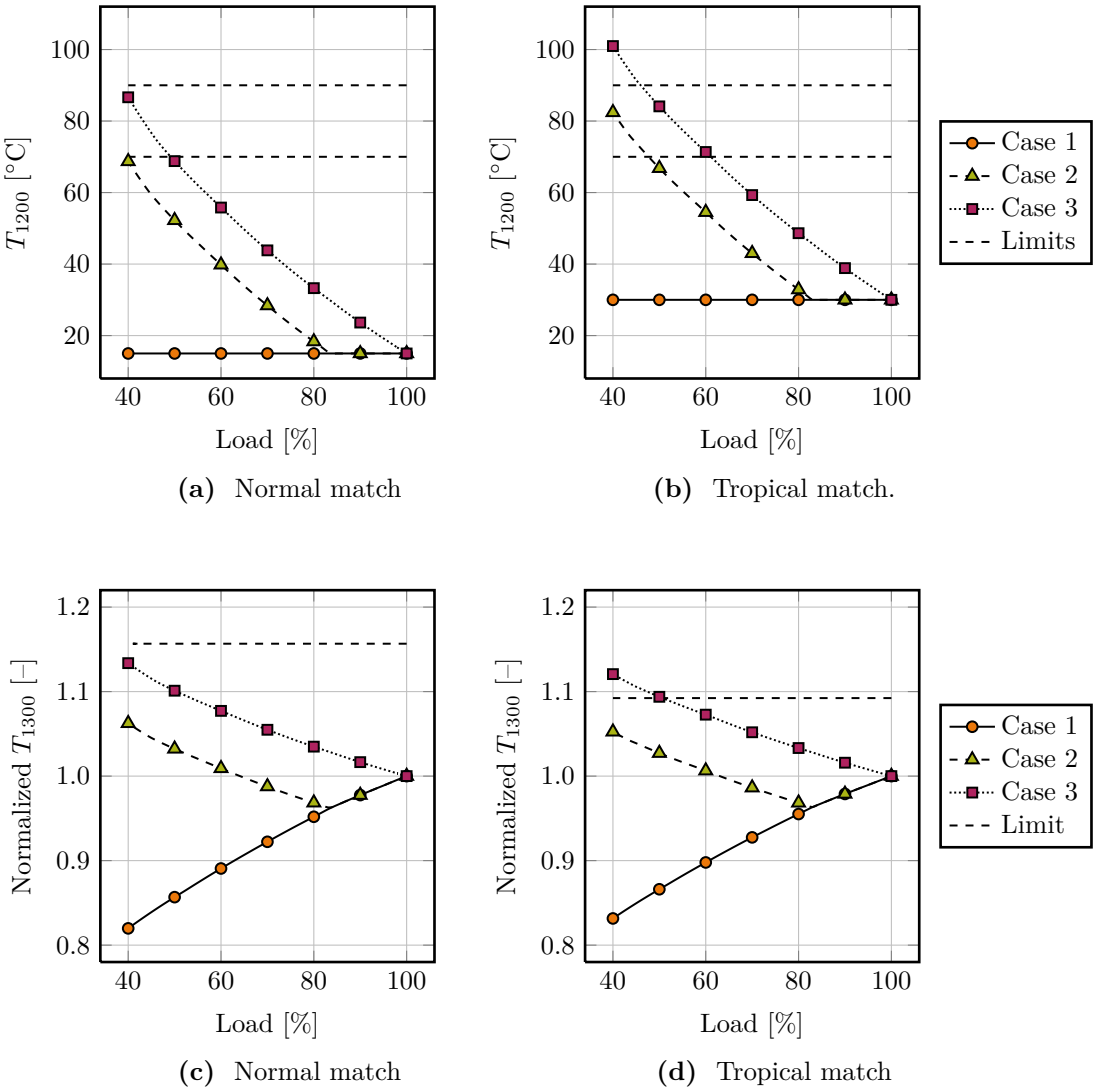

(a) Normal match **(b)** Tropical match.

(c) Normal match **(d)** Tropical match

Figure 4.7. Compressor inlet (a), (b) and outlet (c), (d) temperature as a function of load.

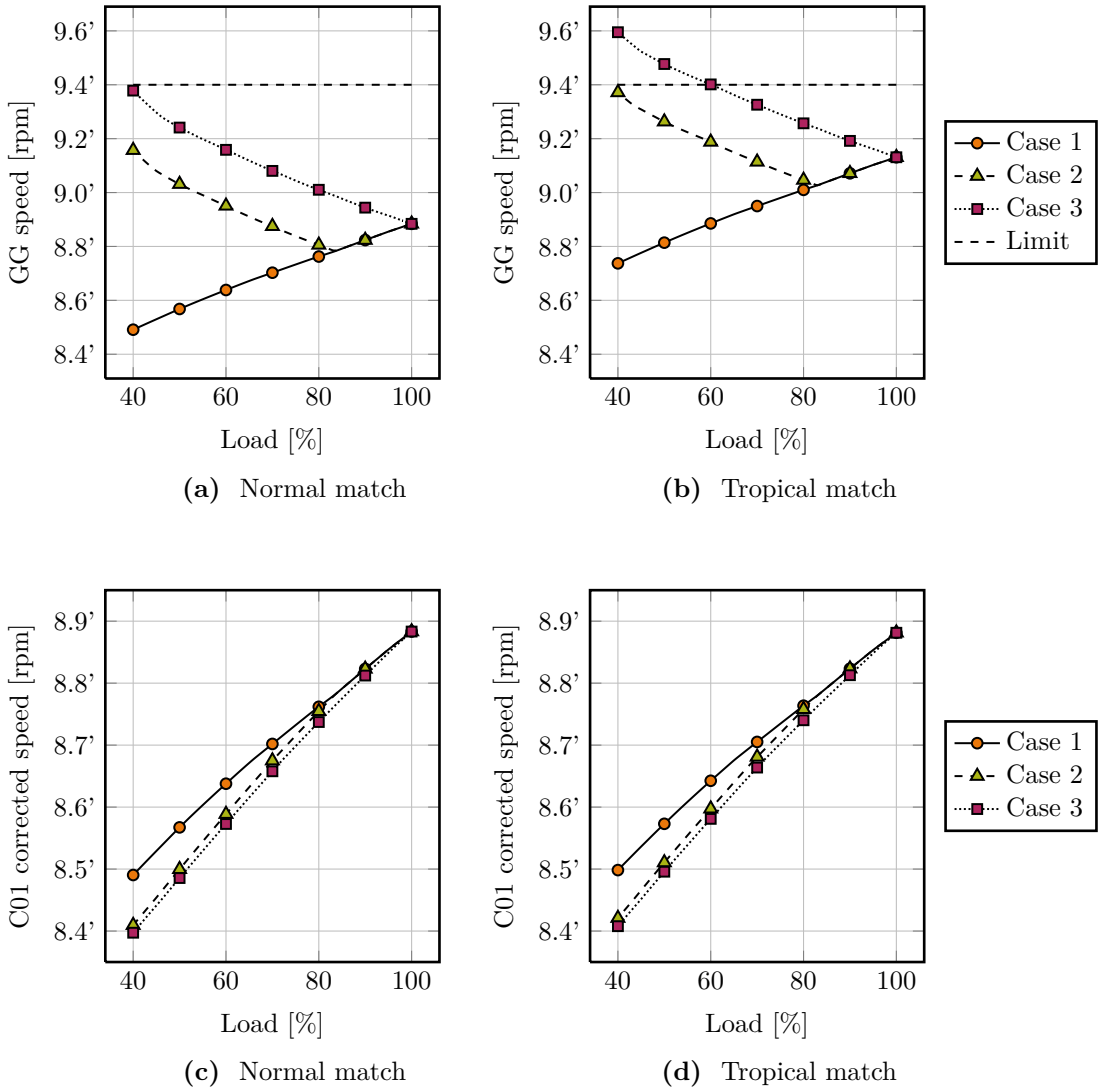

(a) Normal match

(b) Tropical match

(c) Normal match

(d) Tropical match

Figure 4.8. Physical (a), (b) and corrected (c), (d) shaft speed as a function of load.

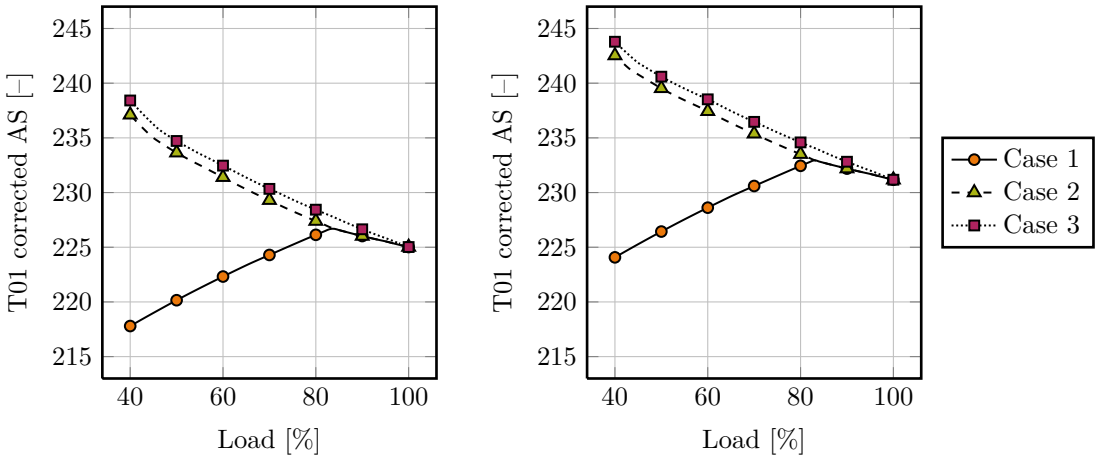

(a) Normal match **(b)** Tropical match

Figure 4.9. Aero speed as a function of load.

4.3 Combined cycle

The results of the combined cycle indicate a rather similar behavior of the gas turbine as in simple cycle since the conditions of the top cycle does not change significantly between the two. In other words the results of Case 1-3 do not differ a lot from the results in simple cycle.

It should be noted that the load in the cases of the combined cycle does not correspond directly with the load in the cases of the simple cycle as the load is calculated with the total power produced by both cycles in the combined cycle. In other words, 50 % load is not the same power output in the simple and combined cycle.

4.3.1 Cycle efficiency

One difference between the simple and the combined cycle is the results of the total cycle efficiency, Figure 4.10. The bottoming cycle in Case 3 is favored by the higher outlet temperature of the top cycle resulting in a higher total cycle efficiency.

Regarding the newly introduced Case 4 and 5 a higher efficiency is obtained since more energy is available from after the top cycle for the bottoming cycle to absorb because no extraction of exhaust gases occurs at this point in these cases. Another way of explaining this phenomenon is that if less energy is being dumped through the stack, more energy is used in the cycle and thus a higher total cycle efficiency is reached. In Case 4 the efficiency is equal to Case 1 and 2 until EGR is initiated since there is no difference in the cases until this point in the process. In Case 5, however, the efficiency is separate right from the start, in similarity to Case 3.

Particularly noteworthy is the fact that the total cycle efficiency only slightly differs in the tropical match compared to the normal match. In the simple cycle a greater difference was found in the cycle efficiencies between the match types, Figure 4.3. This is due to the temperatures in the gas turbine exhaust and stack. A comparision of these temperatures at 100 % load is presented in Table 4.2. The tropically matched cycle has a higher exhaust temperature resulting in a lower efficiency of the top cycle. However, the bottoming cycle will partly compensate for this by benefiting from the higher exhaust temperature. This is done by increasing steam flow resulting in a higher energy absorption and a lower stack temperature.

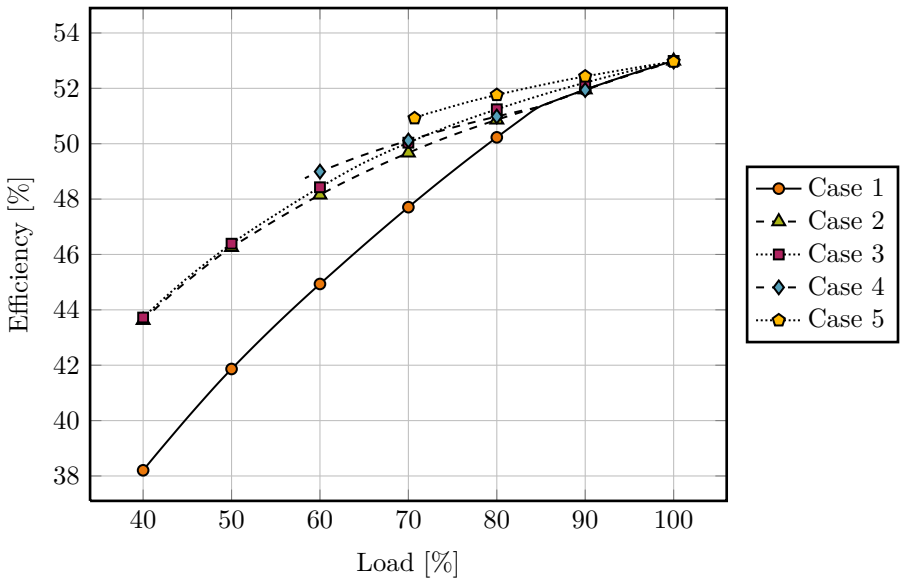

(a) Normal match

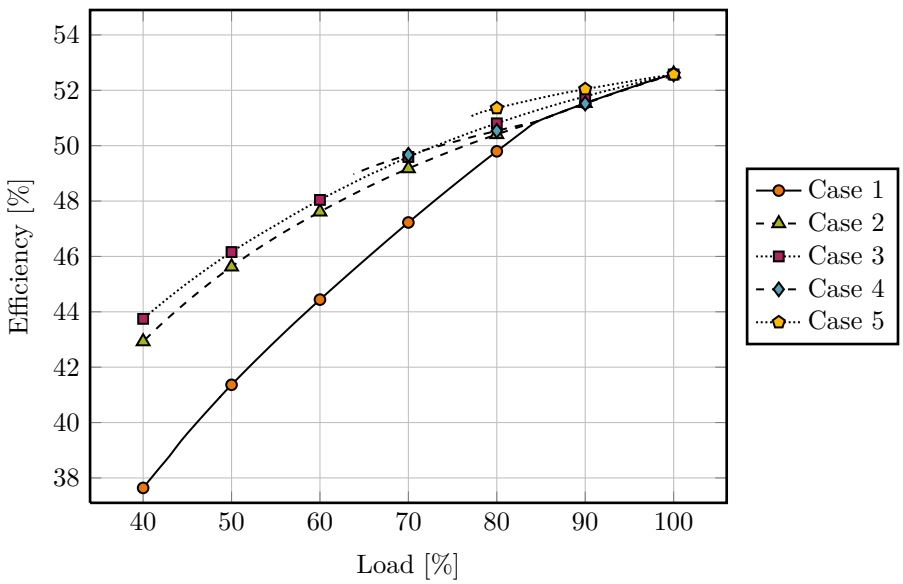

(b) Tropical match

Figure 4.10. Cycle efficiency as a function of load.

Table 4.2. Normalized temperatures in the gas turbine exhaust, 0950, and stack for normal and tropical match at 100 % load.

	T_{0950}	T_{stack}
Normal	1.000	0.235
Tropical	1.015	0.231

The results in Case 4 and 5 are distinctive in the way that the calculations can not be performed on low loads due to the total lack of available oxygen in the combustion chamber outlet. In addition to this, the lower boundary of oxygen content of 8 % is reached already at even higher loads, approximately 62 % and 76 % respectively for the normal match calculations, Figure 4.11. The results yield a rapid decrease in oxygen content with increasing EGR due to lowered load. An exception is noticed in Case 4 that at high loads increase in oxygen content due to a decrease in T_{1520}. The lack of oxygen, and the thereby limit of load variation, greatly limits the use of these methods despite the higher cycle efficiency they offer.

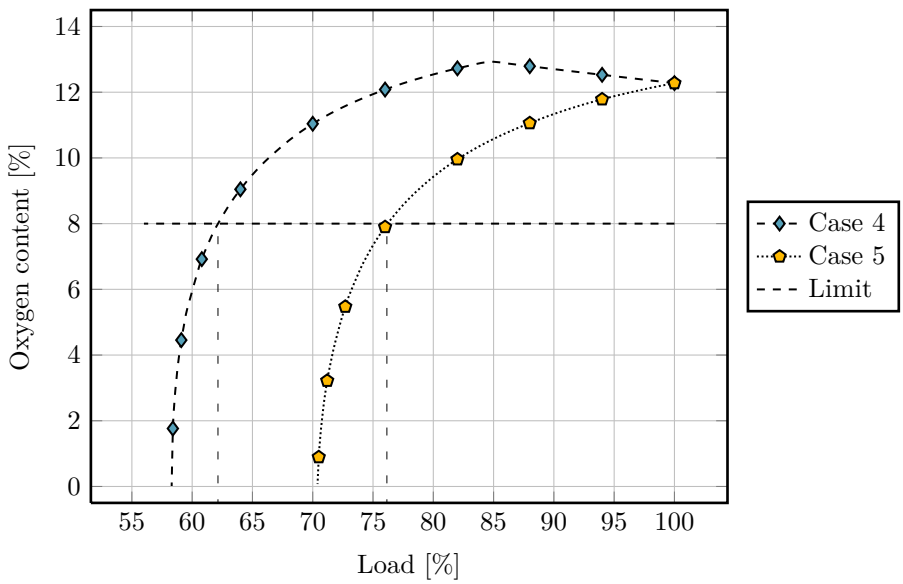

Figure 4.11. Combustion chamber outlet oxygen content as a function of load. The same behavior is found when the gas turbine is tropically matched.

4.3.2 EGR

Since the recirculated exhaust gases in Case 4 and 5 are of significantly lower temperature compared to the other cases, a higher mass flow is needed to satisfy the temperature rise in the compressor inlet. This results in a percentage of EGR a lot higher in these cases, Figure 4.12. It is this rapid rise in EGR that causes the lack of the oxygen content shown in Section 4.3.1.

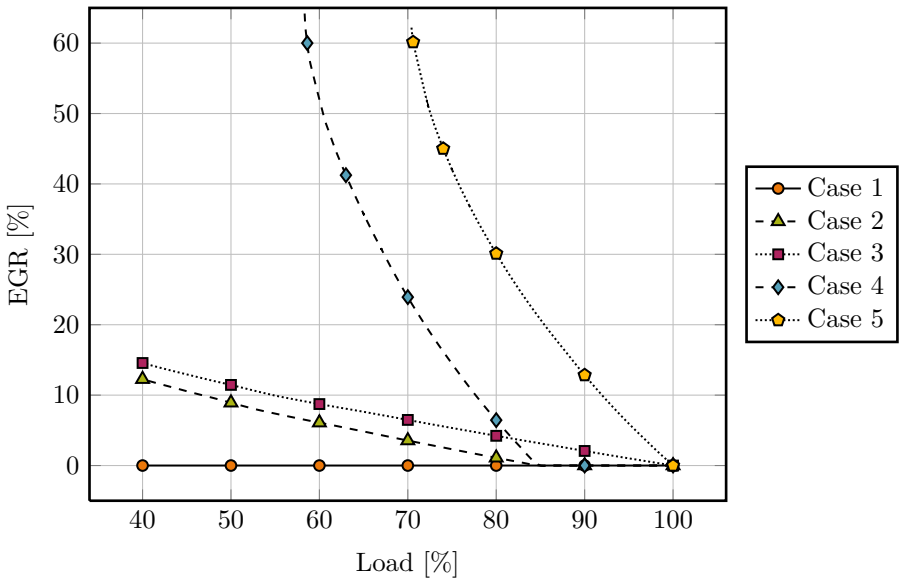

Figure 4.12. EGR as a function of load for normal match. The same behavior is found when the gas turbine is tropically matched.

4.4 Practical aspects

Calculating the pipe pressure loss in the simple and combined cycle for a pressure loss of 13.26 mbar and 0.1 bar in both cases yields a Reynolds number in all cases well above the boundary to ensure a fully turbulent flow. In other words, using the Haaland equation, Equation 2.6b, is the correct approach to estimate the friction factor. The diameter determined varies in the range of 0.3 – 1 m between the cases. For the simple cycle a diameter of 0.6 m would satisfy the pressure loss of 13.26 mbar used in the calculations throughout this thesis while this diameter would result in a pressure drop of approximately 0.1 bar in the combined cycle. This is affecting the cycle performance negatively but is considered to be within an acceptable limit as the loss performance is small compared to the profit of using EGR compared to bleed. Since larger pipes are more expensive there is a profit in settling for a smaller pipe diameter. With this in mind a pipe diameter DN 600 is chosen, a standardized pipe size with a diameter of approximately 600 mm depending on the wall thickness. The results of the calculations are presented in Table 4.3.

Table 4.3. Results of pipe pressure loss calculations.

	Simple cycle 50 % load		Combined cycle 62.13 % load	
Δp_f	0.01326	0.1	0.01326	0.1
Re	690 252	1 091 372	1 468 621	2 191 739
D	0.579	0.344	0.977	0.547
P_{fan}	27.80	191.19	65.07	398.00
η	30.90 %	30.74 %	49.26 %	48.80 %

5

Discussion

Studying the results of this thesis reveals an in general positive impact of EGR implementation. The total cycle efficiency at 50 % load is increased by 3 – 5 percentage points depending on which case of EGR is studied. No particular bad side effects of EGR are found although in some cases different limits of temperature or oxygen content are reached at certain loads. It is recommended that EGR is implemented in the gas turbine cycle to improve performance at part load with the fact in mind that the practical aspects might be a bit troublesome in comparison to the method of bleed.

The method of recirculating heat can be varied so that only the heat and not the actual exhaust gas is recirculated. This is achieved by using a heat exchanger transferring the heat from the exhaust gases to the inlet air. Using this kind of gas to gas heat exchanger would be very space consuming considering the large volume flows present with EGR according to Jonshagen [18]. Instead, there is a possibility of extracting the heat from the feed water of a bottoming cycle in the case of a combined cycle configuration. This would make the heat exchange manageable although it would have negative effects on the total cycle performance. This, since the method is extracting usable heat from the bottoming cycle instead of not used heat from the stack. Also, handling pressurized feed water would require higher standards of the piping and thus a more complicated and expensive recirculation.

5.1 Simple cycle

In general, implementation of EGR has positive effects on the performance of the simple cycle. Both examined cases, Case 2 with lowered mixed TIT to the same level as with bleed and Case 3 with mixed TIT kept high throughout the load variation, result in significantly higher cycle efficiency at part load compared to the method of bleed, Case 1.

The results are similar for the normal as well as for the tropical matching of the power turbine and the overall trends are equal between the compared match cases. However, the higher temperature throughout the machine with the tropical match due to the higher ambient temperature at these conditions results in exceeded limits in Case 3. The temperature limit in the intake air filter is reached in this case for both match types and the temperature limits in the compressor inlet and outlet are also reached when the machine is tropically matched. Furthermore, the limit of shaft speed is exceeded in this case, affecting the lifing negatively as well as the higher TIT also reduces the lifespan. This all together is making Case 3 unsuitable as a method for implementing EGR in the gas turbine cycle.

Although the shaft speed is higher in Case 2 compared to Case 1 at part load, entailing negative influence on lifing as stated in Section 2.4.2, a rotational speed below the limit has to be considered acceptable. With no other limitations reached except for the momentary limit of 70 °C in the intake air filter with loads as low as below 50 %, Case 2 is equal or superior to Case 1 in all examined physical aspects.

5.2 Combined cycle

The overall performance profits from EGR also in the combined cycle configuration. The results of Case 1–3 are rather similar to the results of the simple cycle analysis and as stated in Section 4.3, this is due to the non changing conditions of the top cycle. However, a difference is found in the cycle efficiency were Case 3 results in a higher efficiency due to the higher outlet temperature of the top cycle.

The main differences between the simple and combined cycle occurs in the cases specific for the combined cycle, Case 4 and 5 were Case 5 in similarity with Case 3 results in the highest cycle efficiency. This case is however only applicable at loads above 76 % due to the high percentage of recirculation resulting in low oxygen content making the case nonoptimal as the sole method of EGR implementation. The same applies for Case 4 which is usable at loads above 62 %.

In summary the potential of the combined cycle is greater than for the simple cycle but the limitations restricts its opportunities.

5.3 Conclusion

Regarding the simple cycle Case 2 is the best performing method throughout the complete range of load variation and hence, this would be the recommended way of replacing bleed with EGR to improve the gas turbine's performance at part load. The method of lowering the TIT to a certain level after which it is kept constant due to an increase in EGR affected the cycle performance as expected. The higher temperature in the compressor inlet due to EGR results in a lowered mass flow and a decreased power output with a fixed TIT according to Section 2.4. The analysis yields the somewhat surprising result that a higher TIT results in worse performance. This is however, as explained in Section 4.2.2, because of the lower pressure ratio in this case.

Even though the SGT-750 is not designed to work in a combined gas turbine cycle the results can yield trends and give a hint of how other twin shaft gas turbines adapted for combined cycles would perform. The results of the combined cycle analysis are different than the of the simple cycle. Ultimately the best results would be achieved by combining the methods of EGR since different methods are superior in different ranges of load. By starting with a TIT kept high and recirculating exhaust gases from the stack straight from the start of the load decrease and when the oxygen limit of 8 % is reached, keep the oxygen level at this limit by decreasing the mixed TIT, a maximal cycle efficiency will be achieved. To further lower the load, either the EGR from the stack has to be combined with EGR from after the top cycle or the TIT has to be lowered further, neither of which is examined in this thesis. Alternatively bleed could be used at loads below this point in which case the performance would suffer. It should be borne in mind however that even though this is the case, the performance is significantly improved for higher loads before bleed is initiated.

Conclusively the scope of the thesis is fulfilled. A future-proof model of the SGT-750 for IPSEpro, reading characteristics from text files, has been created. The model is consistent with the performance calculation software at SIT and the minor existing deviation is considered to be within acceptable margins. Furthermore it is considered proven that it is possible to reduce the load of a twin shaft gas turbine by using EGR to maintain a high flame temperature and thus handling the emissions and improving the general performance of the machine. This is the case in a simple cycle as well as in a combined cycle configuration with both normal and tropical matching of the power turbine.

5.4 Sources of error

Regarding the accuracy of the performed calculations the eventual errors are kept at acceptable levels. The following exemplifies parts of the calculations that might led to minor errors.

- The machine is considered to be adiabatic since no heat exchange with the surroundings is taken into account. This might not really be the case of the psychical machine although gas turbines are quite thoroughly insulated. A slight heat loss will occur that is not considered in the calculations that will lead to a better performance of this model compared to the reality.
- Leak in the secondary air system is considered according to SIT standard of performance prediction and evaluation. Perhaps further leakage has to be considered for the losses to be compensated sufficiently.
- Physical losses as for example shaft and generator losses are approximated in the model with proven methods. The losses are calculated from polynomials created at SIT based on extensive experience within the field.
- The results of model validation yield an average deviation below 0.1 % due to errors in gas data. Even though these errors results in a deviation of up to 100 kW of power in certain cases the error is considered to be within the margin or error since the percentage of error is still low.
- Although based on company knowledge and experience the general assumptions made, as for example in the pipe pressure loss calculations, always poses a risk to be possible sources of error.

In addition to these general sources of error it has, during the work of this thesis, arisen some sources of more specific nature.

- The approximation of the electrical and mechanical efficiency of 90 % in the motors driving the EGR fan and the feed water pumps is restrictively set. This might lead to a lower cycle efficiency than actually is the case.
- The pressure drop in the HRSG is set constant to 25 mbar throughout the load variation although a more likely scenario is that it would decrease with lowered load. Furthermore the pressure drop in the intake air filter was not restored to 8 mbar at full load when the model was modified to a combined cycle and was therefore slightly too low during the calculations in this part.

Conclusively some sources of possible error are remaining in the calculations. However, these have little to no impact and the results are therefore considered to be within the margin of error. Also noteworthy is that it is not the results in numbers that are the main scope of this thesis, but the comparison between them.

5.5 Future work

This thesis only covers the impact in EGR on the cycle in general. To continue the research and development process of implementing EGR in the gas turbine cycle the effect on each component needs to be specifically examined. The implementation of EGR also has to be solved practically. A more profound analysis determining exactly what piping and other parts are needed and exactly how the exhaust gases will be extracted and inserted in the cycle has to be done. Furthermore a financial analysis has to be performed to be able to fully determine the profitability of EGR implementation.

An interesting study would be to examine the impact of alternative methods as for example burner bypass. The method of bypassing the pressurized air over the burners was rejected as a method for the SGT-750 due to the can burner setup but a solution might be possible to achieve with further studies on the subject. Regardless of which, the method would have been interesting for other twin shaft gas turbines and could be compared to the results of this thesis.

References

[1] Siemens AG. *Historia*. 2015. URL: http://www.sit-ab.se/01_historia.html. Accessed: 2015-03-23.

[2] H. Cohen, G. F. C. Rogers and H. I. H. Saravanamuttoo. *Gas turbine theory*. 4th edition. Harlow, England: Longman, 1996. ISBN: 0-582-23632-0.

[3] Siemens AG. *Gas Turbine SGT-750*. 2015. URL: http://www.energy.siemens.com/hq/en/fossil-power-generation/gas-turbines/sgt-750.htm#content=Technical%20data. Accessed: 2015-02-12.

[4] K. Tageman. *SGT-750*. Personal interview. Finspång, 2015-02-11.

[5] Siemens Industrial Turbomachinery AB. *SGT-750*. 2010. URL: http://www.sit-ab.se/images/fotoarkiv/SIM00010_coated_20cm.jpg. Accessed: 2015-02-11.

[6] Y. A. Çengel and M. A. Boles. *Thermodynamics: An Engineering Approach*. 4th edition. Boston, USA: McGraw-Hill Higher Education, 2002. ISBN: 0-07-112177-3.

[7] D. F. Young, B. R. Munson, T. H. Okiishi and W. W. Huebsch. *A brief introduction to fluid mechanics*. 4th edition. Hoboken, USA: Wiley, 2007. ISBN: 978-0-470-03962-5.

[8] S. E. Haaland. "Simple and Explicit Formulas for the Friction Factor in Turbulent Pipe Flow". *Journal of Fluids Engineering*, vol. 105, 1983, pp. 89–90. DOI: 10.1115/1.3240948.

[9] P. P. Walsh and P. Fletcher. *Gas turbine performance*. Oxford, England: Blackwell Science, 1998. ISBN: 0-632-04874-3.

[10] K. Jonshagen. *Modern Thermal Power Plants – Aspects on Modelling and Evaluation*. PhD thesis. Department of Energy Sciences, Lund University. 2011.

[11] S. L. Dixon. *Fluid mechanics and thermodynamics of turbomachinery*. 4th edition. Boston, USA: Butterworth-Heinemann, 1998. ISBN: 0-750-67059-2.

[12] A. M. Y. Razak. *Industrial gas turbines performance and operability*. 4th edition. Cambridge, England: Woodhead Publishing, 2007. ISBN: 978-1-84569-205-6.

[13] H. Li, G. Haugen, M. Ditatanto, D. Bernstad and K. Jordal. "Impacts of exhaust gas recirculation (EGR) on the natural gas combined cycle integrated with chemical absorption CO_2 capture technology". *Energy Procedia*, vol. 4, 2011, pp. 1411–1418. DOI: 10.1016/j.egypro.2011.02.006.

[14] J. Nilsson. *SGT-750 inlet casing*. Personal communication. Finspång, 2015-02-10.

[15] R. Andersson. *MGTX Design parameters for bleed and cooling air pipes*. Internal technical report: Confidential. Siemens Industrial Turbomachinery AB, Finspång. 2011.

[16] D. Jonsson. *SGT-750 intake air filter*. Personal communication. Finspång, 2015-03-04.

[17] J. Janczewski. *SGT-750 oxygen content*. Personal interview. Finspång, 2015-02-27.

[18] K. Jonshagen. *EGR with heat exchangers*. Personal interview. Finspång, 2015-03-12.

[19] L. C. Böiers and A. Persson. *Analys i en variabel*. 3rd edition. Lund: Studentlitteratur, 2010. ISBN: 978-9-144-06765-0.

[20] M. Mondejar. *How to create a customized DLL for IPSE pro*. Department of Energy Sciences, Lund University. 2014.

[21] SimTech. *IPSEpro Model Development Kit*. Manual Version 3.1.001, 2000.

[22] M. Sjödin. *SIT Performance Model Definition*. Internal technical report: Confidential. Siemens Industrial Turbomachinery AB, Finspång. 2011.

[23] SimTech. *IPSEpro Advanced Power Plant Library*. Manual Version 9.0.001, 2014.

[24] C. Andersson. *CFD-simulation of exhaust gas recirculation*. Technical report. FS Dynamics. 2010.

[25] O. Lindman. *Piping standards and material*. Personal communication. Finspång, 2015-03-19.

[26] ThyssenKrupp. *Material Data Sheet 1.5415*. 2011. URL: http://www.s-k-h.com/media/de/Service/Werkstoffblaetter_englisch/Kesselrohre_EN/16Mo3_1.5415_engl.pdf. Accessed: 2015-03-20.

[27] R. Astley. *Never gonna give you up*. 1987. URL: https://www.youtube.com/watch?v=dQw4w9WgXcQ. Accessed: 2015-04-17.

A

DLL code

```
#include <windows.h>
#include "stdafx.h"
#include <iostream>
#include <fstream>
#include <string>
#include <vector>
using namespace std;

#define EXTERN_FUNCTION __declspec(dllexport) _stdcall
extern "C" {
  void C01_read();
  void C01_calc(double speed_in, double pi_in);

  double EXTERN_FUNCTION C01_m(double speed_in, double pi_in);
  double EXTERN_FUNCTION C01_dm_dspeed(double speed_in, double pi_in);
  double EXTERN_FUNCTION C01_dm_dpi(double speed_in, double pi_in);
  double EXTERN_FUNCTION C01_eta(double speed_in, double pi_in);
  double EXTERN_FUNCTION C01_deta_dspeed(double speed_in, double pi_in);
  double EXTERN_FUNCTION C01_deta_dpi(double speed_in, double pi_in);
}

// Defining objects
string line;
ifstream C01 ("SGT-750_001.C01");

// Defining vectors and variables
bool breaker_speed, breaker_interp_1, breaker_interp_2, breaker_above,
     breaker_below;
int row_counter, no_of_igv_angles_C01, igv_angle_C01, no_of_speed_lines_C01,
     no_of_lines_per_speed_line_C01;
double m_flow_1, m_flow_2, eta_p_1, eta_p_2, fc_1, fc_2, eta_s_1, eta_s_2;
vector<int> misc_values_C01;
vector<double> speed_lines_C01, m_flow_surge_C01, pi_surge_C01, m_flow_C01, pi_C01,
      eta_p_C01;
double m_flow_return, eta_p_return;
bool C01IsRead = false;
```

```
34 //*********************************************************************//
35 //************************* Read from files ***************************//
36 //*********************************************************************//
37
38 //****************************** Read C01 *****************************//
39
40 void C01_read(){
41
42   if (C01.is_open()) {
43     row_counter = 0;
44
45     // Gets next line
46     while (getline(C01 >> std::ws, line)) {
47
48       // To skip commentary lines
49       if (line[0] != ';') {
50         row_counter++;
51         int pos_start;
52         int pos_end;
53
54         if (row_counter == 10 || row_counter == 11 || row_counter == 12 ||
               row_counter == 13) {
55           pos_start = line.find_first_not_of(' ');
56           misc_values_C01.push_back(atoi(line.substr(pos_start).c_str()));
57
58           if (row_counter == 13) {
59             no_of_igv_angles_C01 = misc_values_C01[0];
60             igv_angle_C01 = misc_values_C01[1];
61             no_of_speed_lines_C01 = misc_values_C01[2];
62             no_of_lines_per_speed_line_C01 = misc_values_C01[3];
63           }
64         }
65
66         if (row_counter >= 14) {
67
68           if ((row_counter-14) % (no_of_lines_per_speed_line_C01+1) == 0) {
69             // speed
70             pos_start = line.find_first_not_of(' ');
71             string temp0a = line.substr(pos_start);
72             pos_end = temp0a.find_first_of(' ');
73             speed_lines_C01.push_back(strtod(line.substr(pos_start, pos_end).c_str
                   (), NULL));
74
75             // m_flow_C01 @ surge
76             string temp0b = temp0a.substr(pos_end);
77             pos_start = temp0b.find_first_not_of(' ');
78             string temp0c = temp0b.substr(pos_start);
79             pos_end = temp0c.find_first_of(' ');
80             m_flow_surge_C01.push_back(strtod(temp0b.substr(pos_start, pos_end).
                   c_str(), NULL));
81
82             // pi_C01 @ surge
83             string temp0d = temp0c.substr(pos_end);
84             pos_start = temp0d.find_first_not_of(' ');
85             string temp0e = temp0d.substr(pos_start);
86             pos_end = temp0e.find_first_of(' ');
87             pi_surge_C01.push_back(strtod(temp0d.substr(pos_start, pos_end).c_str()
                   , NULL));
88           } else {
89             // m_flow_C01
90             pos_start = line.find_first_not_of(' ');
91             string temp1 = line.substr(pos_start);
92             pos_end = temp1.find_first_of(' ');
93             m_flow_C01.push_back(strtod(line.substr(pos_start, pos_end).c_str(),
                   NULL));
```

```
94              // pi_C01
95              string temp2 = temp1.substr(pos_end);
96              pos_start = temp2.find_first_not_of(' ');
97              string temp3 = temp2.substr(pos_start);
98              pos_end = temp3.find_first_of(' ');
99              pi_C01.push_back(strtod(temp2.substr(pos_start, pos_end).c_str(), NULL)
                    );
100
101             // eta_p_C01
102             string temp4 = temp3.substr(pos_end);
103             pos_start = temp4.find_first_not_of(' ');
104             string temp5 = temp4.substr(pos_start);
105             eta_p_C01.push_back(strtod(temp4.substr(pos_start).c_str(), NULL));
106           }
107         }
108       }
109     } C01.close();
110   } C01IsRead = true;
111 }
112
113 //*************************************************************************//
114 //******************** Calculation / Interpolation ********************//
115 //*************************************************************************//
116
117 //****************** Calculation / Interpolation C01 ******************//
118
119 void C01_calc(double speed_in, double pi_in) {
120
121   if(!C01IsRead) {
122     C01_read();
123   }
124
125   breaker_speed = false;
126   breaker_interp_1 = false;
127   breaker_interp_2 = false;
128   breaker_above = false;
129   breaker_below = false;
130
131   // Iterates all speed lines
132   for (int i = 0; i < no_of_speed_lines_C01 - 1; i++) {
133
134     // Checks if speed_in is between the current speed lines
135     if(speed_in < speed_lines_C01[i+1] && !breaker_speed) {
136
137       // Sets b true to break loop
138       breaker_speed = true;
139
140       // Checks if pi_in is above surge line
141       if (pi_in > pi_surge_C01[i]) {
142         breaker_above = true;
143       }
144
145       // Checks if pi_in is below characteristics
146       else if (pi_in < pi_C01[no_of_lines_per_speed_line_C01 * (i+1) - 1]) {
147         breaker_below = true;
148       }
149
150       // If pi_in is i characteristics
151       if (!breaker_above && !breaker_below) {
152
153         for (int i1 = no_of_lines_per_speed_line_C01 * i; i1 < (
                no_of_lines_per_speed_line_C01 * (i+1)) && !breaker_interp_1; i1++) {
154
155           if(pi_in > pi_C01[i1+1]) {
156
```

```
157             double pi_interp_1 = (pi_in - pi_C01[i1]) / (pi_C01[i1+1] - pi_C01[i1])
                    ;
158             m_flow_1 = pi_interp_1 * (m_flow_C01[i1+1] - m_flow_C01[i1]) +
                    m_flow_C01[i1];
159             eta_p_1 = pi_interp_1 * (eta_p_C01[i1+1] - eta_p_C01[i1]) + eta_p_C01[
                    i1];
160
161             breaker_interp_1 = true;
162           }
163         }
164
165         for (int i2 = no_of_lines_per_speed_line_C01 * (i+1); i2 < (
                no_of_lines_per_speed_line_C01 * (i+2)) && !breaker_interp_2; i2++) {
166
167           if(pi_in > pi_C01[i2+1]) {
168
169             double pi_interp_2 = (pi_in - pi_C01[i2]) / (pi_C01[i2+1] - pi_C01[i2])
                    ;
170             m_flow_2 = pi_interp_2 * (m_flow_C01[i2+1] - m_flow_C01[i2]) +
                    m_flow_C01[i2];
171             eta_p_2 = pi_interp_2 * (eta_p_C01[i2+1] - eta_p_C01[i2]) + eta_p_C01[
                    i2];
172
173             breaker_interp_2 = true;
174           }
175         }
176       }
177
178       // Calculates m_flow_return & eta_p_return
179       if (breaker_above || breaker_below) {
180         m_flow_return = 0;
181         eta_p_return = 1;
182       } else {
183         m_flow_return = (speed_in - speed_lines_C01[i]) / (speed_lines_C01[i+1] -
                speed_lines_C01[i]) * (m_flow_2 - m_flow_1) + m_flow_1;
184         eta_p_return = (speed_in - speed_lines_C01[i]) / (speed_lines_C01[i+1] -
                speed_lines_C01[i]) * (eta_p_2 - eta_p_1) + eta_p_1;
185       }
186     }
187   }
188 }
189
190 //*************************************************************************//
191 //************************ Extern functions ************************//
192 //*************************************************************************//
193
194 //************************ Extern functions C01 ************************//
195
196 double EXTERN_FUNCTION C01_m(double speed_in, double pi_in) {
197   C01_calc(speed_in, pi_in);
198   return m_flow_return;
199 }
200
201 double EXTERN_FUNCTION C01_dm_dspeed(double speed_in, double pi_in) {
202   double f_x = C01_m(speed_in, pi_in);
203   double h = 0.001 * speed_in;
204   double f_x_h = C01_m(speed_in + h, pi_in);
205   return (f_x_h - f_x) / h;
206 }
207
208 double EXTERN_FUNCTION C01_dm_dpi(double speed_in, double pi_in) {
209   double f_x = C01_m(speed_in, pi_in);
210   double h = 0.001 * pi_in;
211   double f_x_h = C01_m(speed_in, pi_in + h);
212   return (f_x_h - f_x) / h;
```

```
213 }
214
215 double EXTERN_FUNCTION C01_eta(double speed_in, double pi_in) {
216   C01_calc(speed_in, pi_in);
217   return eta_p_return;
218 }
219
220 double EXTERN_FUNCTION C01_deta_dspeed(double speed_in, double pi_in) {
221   double f_x = C01_eta(speed_in, pi_in);
222   double h = 0.001 * speed_in;
223   double f_x_h = C01_eta(speed_in + h, pi_in);
224   return (f_x_h - f_x) / h;
225 }
226
227 double EXTERN_FUNCTION C01_deta_dpi(double speed_in, double pi_in) {
228   double f_x = C01_eta(speed_in, pi_in);
229   double h = 0.001 * pi_in;
230   double f_x_h = C01_eta(speed_in, pi_in + h);
231   return (f_x_h - f_x) / h;
232 }
```

B

Model deviation

Table B.1. Deviation of results from model in IPSEpro and GTPerform.

	ISO conditions	T_{amb} 45 °C	T_{amb} -25 °C	P_{gen} 22 MW
1200				
p	0.00 %	0.00 %	0.00 %	0.00 %
T	0.00 %	0.00 %	0.00 %	0.00 %
h	0.09 %	0.09 %	0.31 %	0.09 %
$\dot{m}$	0.08 %	0.18 %	0.01 %	0.01 %
1300				
p	0.06 %	0.07 %	-0.05 %	-0.06 %
T	-0.06 %	-0.06 %	-0.15 %	-0.11 %
h	0.00 %	0.01 %	-0.08 %	-0.05 %
$\dot{m}$	0.08 %	0.18 %	0.01 %	0.01 %
1500				
p	0.07 %	0.17 %	-0.06 %	-0.05 %
T	0.00 %	0.00 %	0.00 %	0.00 %
h	0.10 %	0.10 %	0.12 %	0.10 %
$\dot{m}$	0.07 %	0.17 %	-0.07 %	-0.05 %
1520				
p	0.07 %	0.17 %	-0.06 %	-0.05 %
T	0.00 %	0.00 %	0.00 %	0.00 %
h	0.09 %	0.09 %	0.10 %	0.09 %
$\dot{m}$	0.07 %	0.17 %	-0.06 %	-0.04 %
0500				
p	0.10 %	0.20 %	-0.02 %	-0.02 %
T	0.10 %	0.09 %	0.09 %	0.09 %
h	0.14 %	0.14 %	0.15 %	0.13 %
$\dot{m}$	0.07 %	0.17 %	-0.06 %	-0.04 %
Shaft 01				
N	0.01 %	0.03 %	0.02 %	0.00 %
P	-0.08 %	-0.18 %	0.05 %	0.04 %
Shaft 00				
N	0.00 %	0.00 %	0.00 %	0.00 %
P	0.20 %	0.39 %	0.00 %	0.00 %
Gear 00				
P_{loss}	0.01 %	0.02 %	0.00 %	0.00 %
Generator 00				
P	0.20 %	0.40 %	0.00 %	0.00 %
P_{loss}	0.16 %	0.18 %	0.00 %	0.00 %
Average	**0.057 %**	**0.098 %**	**0.063 %**	**0.045 %**